HHS Public Access

Author manuscript

Compr Physiol. Author manuscript; available in PMC 2016 October 01.

Published in final edited form as:

Compr Physiol. ; 5(4): 1877–1909. doi:10.1002/cphy.c140067.

Physiological Implications of Myocardial Scar Structure

WJ Richardson[1,4], **SA Clarke**[1], **TA Quinn**[2], and **JW Holmes**[1,3,4]

[1]Department of Biomedical Engineering, University of Virginia; Charlottesville, Virginia, USA

[2]Department of Physiology and Biophysics, Dalhousie University; Halifax, Nova Scotia, Canada

[3]Department of Medicine, University of Virginia; Charlottesville, Virginia, USA

[4]Robert M. Berne Cardiovascular Research Center, University of Virginia; Charlottesville, Virginia, USA

Abstract

Once myocardium dies during a heart attack, it is replaced by scar tissue over the course of several weeks. The size, location, composition, structure and mechanical properties of the healing scar are all critical determinants of the fate of patients who survive the initial infarction. While the central importance of scar structure in determining pump function and remodeling has long been recognized, it has proven remarkably difficult to design therapies that improve heart function or limit remodeling by modifying scar structure. Many exciting new therapies are under development, but predicting their long-term effects requires a detailed understanding of how infarct scar forms, how its properties impact left ventricular function and remodeling, and how changes in scar structure and properties feed back to affect not only heart mechanics but also electrical conduction, reflex hemodynamic compensations, and the ongoing process of scar formation itself. In this article, we outline the scar formation process following an MI, discuss interpretation of standard measures of heart function in the setting of a healing infarct, then present implications of infarct scar geometry and structure for both mechanical and electrical function of the heart and summarize experiences to date with therapeutic interventions that aim to modify scar geometry and structure. One important conclusion that emerges from the studies reviewed here is that computational modeling is an essential tool for integrating the wealth of information required to understand this complex system and predict the impact of novel therapies on scar healing, heart function, and remodeling following myocardial infarction.

Introduction

Over a million Americans suffer a heart attack each year, and most now survive the initial event. Once myocardium dies during a heart attack, it is replaced by scar tissue over the course of several weeks. The size, location, composition, structure and mechanical properties of the healing scar are all critical determinants of the fate of patients who survive the initial infarction. Initial depression of left ventricular pump function depends strongly on infarct size, as does the long-term risk of left ventricular remodeling that commonly leads to heart failure following infarction; yet even identically sized infarcts in different locations carry different prognoses. Some infarcts cannot withstand the mechanical loads placed on them and rupture in the first few days, a catastrophic and usually fatal complication. Others gradually stretch and thin (a process termed infarct expansion), increasing wall stresses and

accelerating ventricular remodeling and the development of heart failure. While the central importance of scar structure in determining pump function and remodeling has long been recognized, it has proven remarkably difficult to design therapies that improve heart function or limit remodeling by modifying scar structure. Many exciting new therapies are under development, but predicting their long-term effects requires a detailed understanding of how infarct scar forms, how its properties impact left ventricular function and remodeling, and how changes in scar structure and properties feed back to affect not only heart mechanics but also electrical conduction, reflex hemodynamic compensations, and the ongoing process of scar formation itself. In this article, we will first review the scar formation process following an MI and the evolution of collagen content and alignment, collagen fiber orientation, and scar geometry during infarct healing. We will then discuss measures of heart function typically employed following infarction, with specific attention to their interpretation in the setting of a healing infarct. Then, we will present implications of infarct scar geometry and structure for both mechanical and electrical function of the heart. Finally, we will close with a discussion of therapeutic interventions that aim to modify scar geometry and structure, and their effects on heart function and remodeling.

Scar Formation and Remodeling Following Myocardial Infarction

Overview of Infarct Healing

Myocardial infarction (MI) occurs when prolonged reduction in blood flow to a region of the heart results in permanent death of myocytes. Over the following days and weeks, the dead myocytes are gradually replaced by a collagenous scar. This progression of myocardial wound healing following infarction is a dynamic process generally divided into three stages: inflammation/necrosis, fibrosis/proliferation, and long-term remodeling/maturation (Figure 1) (59, 112, 126).

Inflammatory Phase—The necrotic or inflammatory phase of infarct healing occurs over the first few days in small animals and the first week or more in large animals and humans (57, 69, 70, 293). After prolonged ischemia, cardiomyocytes undergo necrosis followed by a wound healing cascade wherein a variety of inflammatory cells including neutrophils, macrophages, and lymphocytes invade the ischemic zone beginning within hours of injury, peaking several days later at several thousand cells/mm^2 in small animals, with lower numbers lingering for a week or longer (70, 293). These cells play central roles in the wound healing process including both remodeling and signaling functions. Structural remodeling of the ischemic area is initiated as inflammatory cells and necrotic myocytes secrete and activate matrix metalloproteinases (MMPs) including MMP1, 2, 3, 7, 8, 9, 12, 13, and 14 (160, 267, 297). These proteinases degrade cell and matrix material aiding phagocytic macrophages in the resorption of necrotic tissue. This early proteinase activity is also thought to disrupt the collagen fibers and struts that supported cardiomyocyte structure in the once-healthy myocardium (286).

While new collagen accumulation is not apparent for several days after the initial injury, as necrotic myocytes are resorbed, a provisional granulation tissue consisting of fibrin, fibronectin, laminin, glycosaminoglycans (GAGs), and other matrix is laid in their place (57, 160, 265). Figure 1B presents data from 25 studies that reported mRNA or protein levels of

various extracellular matrix components during infarct healing in small animals, averaged across functional groups of similar molecules and fitted to highlight the temporal dynamics of changes in each group. Rapid increases in GAGs and provisional matrix molecules begin within 24 hours after infarction, and resolve during the fibrotic phase. These matrix proteins maintain temporary structural support until the myofibroblasts upregulate the secretion of fibrillar collagen that will ultimately become the primary structural constituent of cardiac scar tissue.

In addition to producing proteinases, inflammatory cells upregulate the release of a myriad of signaling cytokines, growth factors, and hormones including transforming growth factor β, interleukins 1, 2, 6, and 10, tumor necrosis factor α, interferon γ, chemokines of the CC and CXC families, angiotensin II, norepinephrine, endothelin, natriuretic peptides, and platelet-derived growth factors (57, 160, 249, 285, 299). The details of this complex signaling mileau have been extensively reviewed elsewhere (56, 77); here, we note only that these molecules are essential to the recruitment and activation of fibroblasts as the healing process transitions to its next stage: fibrosis.

Fibrotic Phase—The fibrotic or proliferative phase of healing lasts one to several weeks (57, 69, 70, 293), and is dominated by the actions of myofibroblasts. By number, cardiac fibroblasts are the most abundant cell type in the healthy heart (126, 163). In an infarct zone, their concentration increases through a combination of migration from surrounding myocardium, proliferation, and differentiation of diverse cell types into activated myofibroblasts, including pericytes, smooth muscle cells, endothelial cells, mesenchymal stem cells, and circulating fibrocytes (56, 93, 163). Myofibroblasts are characterized by increased α-smooth muscle actin expression that generally accompanies elevated migration and contractile force as well as increased expression of matrix proteins (56). Beginning several days after MI, myofibroblasts can increase 20-fold in abundance to reach several thousand cells/mm^2 around 1 week in small animals, and persist at high levels for several weeks (70, 293).

Inflammatory cell expression of MMPs begins to wane a few days after MI, just as myofibroblast expression of pro-collagen (predominantly type I and III but also IV and VI) ramps up drastically, peaking roughly 1 week post infarction before falling back to baseline (29, 47, 182, 203, 250, 292, 300). This transient expression can generate upwards of 10-fold increases in myocardial collagen content, which plateaus several weeks to months after MI (Figure 1B) (21, 47, 99, 122–124, 126, 168, 175). Collagen content is the result of a highly regulated balance between the secretion of collagen and the activation of MMPs and tissue inhibitor of MMPs (TIMPs); thus, steady-state collagen levels can be influenced by a number of chemical and mechanical conditions as discussed in the Therapeutic Modification section below. More extensive reviews of post-MI MMP and TIMP activity can be found in Creemers (51), Lindsey (160), and Vanhoutte (267). During the period when collagen content is increasing most rapidly, reports also show transient increases in the abundance of a number of matricellular proteins (tenascin-C, thrombospondin, osteopontin, periostin, SPARC) that play important structural as well as signaling roles in developing scar (reviewed previously (57, 160, 169, 240)). Supporting their importance, genetic knockout of several of these proteins increases the risk for infarct rupture and mortality (163, 172).

Remodeling Phase—The final stage of infarct scar formation is often termed the remodeling or maturation phase and lasts several weeks in small animals and months in large animals and humans (57, 69, 70, 293). During this time, apoptosis of myofibroblasts slightly reduces cell numbers in the infarct, but a moderate population persists (24, 126, 249). While collagen content begins to stabilize, the scar matures via a steady increase in collagen crosslinking (Figure 1B). In addition to post-MI increases in expression of the cross-linking enzyme lysyl oxidase, the accumulation of cross-links hydroxlysylpyridinium and hydroxylysylpyridinoline as well as the secretion of proteoglycans like decorin and biglycan, which bind to collagen and regulate fibrillogenesis and fiber diameters, continue during this phase (59, 62, 73, 156, 163, 175, 272, 283, 291, 300). These organizational changes in collagen matrix seem to occur at a slower but steady rate that continues longer than the relatively quick initial accumulation of collagen content (62, 73, 122, 272, 300).

Differences Among Experimental Models—The infarct healing process follows the same general pattern across a variety of experimental models. However, there are some important differences between these various models that deserve mention, especially when seeking to extend experimental findings to clinical therapies. The most obvious is that each phase proceeds faster in small animal models (mice and rats) compared to large animals (pigs, dogs, sheep) and humans (57, 69, 70, 293). Another potentially important difference is that collagen content increases are typically lower in rats than in larger animals and patients (averages: rat 6x, dog 11x, sheep 8x, patient 9x pre-infarct value) (21, 47, 99, 122–124, 168, 175). Potentially related to these differences in collagen content, it is well-known that the mouse MI model produces a thin scar that is extraordinarily prone to rupture, relative to other species (80). Thus, the mouse model is commonly selected for rupture studies, but information on other post-infarction remodeling processes from mouse models may have significant limitations for understanding remodeling in larger animals and humans.

The most common experimental approach for generating a myocardial infarction is to induce ischemia through some form of coronary artery ligation or occlusion (138). A difficulty with this technique is that it results in highly variable infarct size, in part due to individual variability in coronary anatomy and the extent of collaterals; as a result, ischemic injury studies can require large cohorts of animals and/or post-hoc size-matching for data analysis (138). Another technique that has been utilized in multiple species is cryo-injury, in which a liquid nitrogen-cooled probe is held against the epicardium long enough to induce cell death (25, 75, 247). In contrast to ischemic infarction, cryo-infarction offers excellent control over scar size, shape, and location, thereby enabling experimental consistency. Cryo-infarcts are typically non-transmural, a feature which may confound some types of analyses but has also been employed for investigating border-zone properties (247). Although it is unclear what fraction of resident fibroblasts survive the ischemic period in a traditional ligation model, it seems likely that cryo-injury kills most of the fibroblasts in the infarct zone, which may alter subsequent healing. Another important difference from ischemic injury is that cryo-injury does not block flow through coronary vessels, allowing the injured zone to become reperfused, which as discussed in the next paragraph may affect the healing process.

As clinical reperfusion via thrombolytics and percutaneous coronary intervention began to show benefit and was adopted into standard practice, many groups shifted toward ischemiareperfusion animal models in order to better approximate the clinical situation following early intervention. Studies have identified several differences between reperfused and non-reperfused infarcts. During ischemic infarction, the spatial distribution of myocyte death spreads as a wavefront moving in the radial direction, generally taking ~6 hours to overtake most of the area at risk and kill the majority of the myocytes that will ultimately die (222). Reperfusion within less than 6 hours halts this wavefront and therefore results in smaller and non-transmural infarcts (221). Weeks later, reperfused infarcts remain thicker and smaller in the circumferential-longitudinal plane (266). Additionally, early reperfusion has been shown to accelerate resorption of necrotic tissue, increase the number of inflammatory cells, increase the numbers of blood vessels, and decrease the number of myofibroblasts within the wound (221, 266). This acceleration of inflammation kinetics is presumably due to reperfused flow increasing the rate at which circulating inflammatory cells reach the infarct. Structurally, these changes result in more surviving myocytes and less collagen density in the infarct area, as well as lower density of cross-links within the collagen matrix (49).

Mature Scar Structure

Fibrillar collagen is the most abundant structural component of infarct scar tissue and a critical determinant of mechanical properties across diverse tissues (73, 252). Thus, many studies of infarct structure have focused on quantifying features of the fibrillar collagen including collagen content, collagen crosslinking, collagen orientation, and the degree of collagen alignment. Collagen content can be assessed both biochemically and morphologically. For biochemical assessment, hydroxyproline, a major component of fibrillar collagen, is commonly used as a proxy measure of content since it can easily be quantified using radiometric or colorimetric assays. Morphologic assessment usually employs either picrosirius red (PSR) staining of tissue sections, polarized light microscopy, or a combination of both (287, 297). Collagen appears bright red in PSR-stained sections, is naturally birefringent and therefore bright under polarized light, and is the sole tissue component that exhibits both those qualities, allowing automated separation of collagen from other tissue components in digital images (73, 287). Nonlinear optical microscopy has emerged recently as an increasingly popular collagen imaging modality (44). The molecular structure of type I collagen enables second-harmonic generation (SHG), often achieved via two-photon excitation, which allows for *in vivo* imaging of cardiac scar up to several hundred micrometers in depth (38).

Techniques such as polarized microscopy and SHG provide information not only on collagen content but also on collagen alignment and organization. This structural information is typically displayed using histograms and quantified in terms of both the average orientation of a particular field, section, or sample and the strength of co-alignment of the collagen fibers. Because measured orientations have a limited range (0° and 180° denote the same orientation), standard averaging and statistics are inappropriate when analyzing fiber orientation data. Instead, researchers generally utilize circular statistics to calculate a mean angle of orientation as well as an alignment index, the most common being

mean vector length (MVL, 0 = no alignment, 1 = perfect alignment) or its related converse, angular standard deviation (0 = perfect alignment) (298).

Collagen Content and Crosslinking—After weeks to months of healing, mature scar is composed predominantly of fibrillar collagen. Collagens I, III, IV, and VI all increase post-infarction but I and III show the most dramatic increases and remain the predominant scar matrix components, in that order (18, 47, 185). The steady-state content of collagen varies, with most reports measuring 5-15 fold increases in hydroxyproline from pre-infarct to chronic infarct tissue (21, 47, 99, 122–124, 168, 175). Even after normalizing by collagen content, the density of hydroxylysylpyridinium and hydroxylysylpyridinoline covalent cross-links in mature scar can increase 2-fold or more in rats compared to pre-infarction (73, 175, 272, 300). As described above, mature infarct scar also contains elevated concentrations of a range of collagen-associated proteins including SPARC, decorin, biglycan, and others (Figure 1B) (163).

Collagen Orientation and Alignment—Historically, gross and microscopic examination of myocardial scar tissue has usually been performed in short-axis rings or sections cut perpendicular to the long axis of the left ventricle (LV). Cutting the LV into short-axis rings is particularly useful for visualizing the size and transmural extent of healing infarcts, and corresponds nicely to the images typically obtained from echocardiography and magnetic resonance imaging (MRI). In such sections, it is apparent that collagen is arranged in concentric layers or shells, like the layers of an onion (Figure 2); very few collagen fibers run radially (75, 288). Quantitative measures of collagen alignment therefore reveal high alignment in the circumferential direction.

However, the collagen structure in a healing infarct is of interest primarily because collagen fibers are the major load-bearing elements in the scar. These fibers resist tension very effectively, providing the structural basis for the exponential stress-strain curve observed when myocardial scar is tested in tension (see Infarct Material Properties below); however, they buckle or coil under compression, providing very little resistance. Therefore, from a mechanics perspective, it is the orientation of collagen within each plane or shell parallel to the epicardial surface (the circumferential-longitudinal plane) that is most important, because the scar is under tension in this plane and compression in the radial direction. Recent studies focusing on collagen orientation in the circumferential-longitudinal plane have shown a surprising variety of collagen fiber orientations and degrees of alignment in different experimental models.

Examining picrosirius-stained sections under polarized light microscopy, Holmes and Covell quantified collagen alignment in pig infarct scar tissue 3 weeks after permanent ligation (113). They found a high degree of anisotropy with strongest fiber alignment (MVL = 0.9) at the midwall and somewhat weaker alignment near the endo- and epicardium. Fiber orientation varied transmurally as well, following a similar pattern as native myocardium but across a narrower range (normal myofiber orientation ranged from −50° at the epicardium to +60° at the endocardium, while mean collagen fiber orientation ranged from −50° to +10°). In stark contrast to the anisotropic structure of pig infarcts, Fomovsky and colleagues used similar methods to examine collagen fiber structure at a range of time points following

permanent ligation in the rat and found very low average fiber alignment (MVL = 0.1 to 0.25) reflecting nearly isotropic structure at all depths and time points (73). In a follow-up study using cryoinfarction to control infarct location, Fomovsky et al. showed that cryo-infarcts at the apex of rat hearts developed minimal collagen alignment at 3 weeks (MVL = 0.1), similar to the rat ligation model, whereas cryo-infarcts at the LV equator showed a higher degree of alignment (MVL = 0.4), similar to the pig ligation model (75). Furthermore, Fomovsky showed that the collagen structure across these different experimental models correlated with regional mechanics (Figure 3): apical infarcts that ultimately developed isotropic collagen structures stretched similarly in the circumferential and longitudinal directions early after infarction, while equatorial infarcts that developed aligned collagen stretched primarily in the circumferential direction. The same group developed an agent-based model to simulate the integrated effects of mechanical environment, local extracellular matrix orientation, chemokine gradients, and other factors on scar formation following myocardial infarction; the model successfully reproduced not only their rat cryo-infarct data but also the transmural trends in collagen fiber orientation in healing pig infarcts discussed above (230).

Surviving Myocytes—In the healed infarct, surviving muscle fibers are widely separated and insulated by connective tissue. However, as discussed under Electrical Implications of Scar Structure below, these myocytes may still play an important role in determining features of electrical propagation in and around the infarct and thereby the risk of post-infarction arrhythmias. A recent high-resolution reconstruction (1 μm^3 voxels) of myocyte and collagen organization in transmural rat ventricular tissue samples showed that lateral coupling between myocytes decreases by ~65% over the first 250 μm of the border-zone, but sparsely connected networks of surviving myocytes do exist within the scar (232). While most of these strands, some as little as one cell thick, terminate within the border-zone, some pass transmurally through the infarct, connecting normal myocardium to surviving sub-endocardial and sub-epicardial layers.

Geometric Remodeling: Thinning, Expansion, and Compaction—In addition to composition and organization, scar geometry is a key property of infarct structure. In an important early study of infarct remodeling, Hutchins and Bulkley examined hearts from patients who died within 30 days post-infarction and observed two apparent dimension changes of the infarcted zone: thinning in the radial direction and dilation in the circumferential direction (116). They termed this pattern of remodeling infarct expansion, and qualitatively identified expansion in 59% of infarcts. In a second autopsy study, Schuster and Bulkley examined hearts obtained within 21 days of MI, qualitatively identified expansion in 49% of infarcts, and associated the presence of expansion with a highly increased probability for rupture (239). In an important quantitative clinical study, Eaton and colleagues collected serial echo images for ~2 weeks post-MI and measured endocardial segment lengths in short axis images (65). On average, these lengths indeed increased over the observation period, and the presence of infarct expansion was associated with more aggressive progression to heart failure and increased mortality over the following months. To identify the mechanisms underlying acute infarct expansion, Weisman and colleagues measured cellular number, density, cross-sectional area, and length within short-

axis histological sections of 1, 2, and 3 day-old infarcted and sham rat ventricles (280). They concluded that acute infarct expansion resulted predominantly from permanent myocyte slippage and rearrangement. A number of other studies across a variety of species have since supported these early findings of an abrupt circumferential dilation of the injured zone within the first few hours after the induction of infarction (28, 66, 132, 157, 178, 195, 271, 273).

At longer times after infarction, infarct thinning remains a consistent and prominent feature of geometric remodeling. Regardless of species and measurement technique, studies have reported progressive scar thinning to an average of ~60% of initial thickness over several months and in some studies to as low as 20% (53, 65, 68, 70, 110, 114, 122, 124, 183, 188, 223, 225). By contrast, long-term studies of in-plane dimensions find a wide range of patterns, from continuing expansion to dramatic compaction (a reduction in one or both in-plane dimensions) (Figure 4). As mentioned above, Eaton et al. reported progressive increases in patient infarct endocardial segment lengths for ~2 weeks after infarction (65). More recently however, Hillenbrand and colleagues used late-enhancement MRI to image 30 MI patients within 12 hours of symptoms and again 5, 12, and ~90 days later (110). Over that time, infarct area in the circumferential-longitudinal plane actually compacted ~9%. This expansion vs. compaction discrepancy has also been reported in dogs: Jugdutt and colleagues reported a 56% increase in infarct-containing segment lengths from 2 days to 6 weeks in a dog ligation model (infarct segment demarcated by papillary muscle landmarks in 2D echo images), whereas Theroux and colleagues reported a 34% decrease from 2 days to 4 weeks in circumferential lengths assessed via implanted pairs of ultrasonic crystal length gauges (124, 258). As discussed under Measures of Post-Infarction Function below, *in vivo* measurements of remodeling can be difficult to interpret because pressures, geometry, and material properties are all changing at once. Accordingly, many experimental studies have examined geometric changes in an unloaded configuration (i.e., arrested, excised, and fixed under zero pressure); such studies are much more likely to report progressive compaction over time (Figure 4B). For example, Fishbein and colleagues induced MI in rats via ligation, then excised, fixed, sectioned, and stained ventricles in short axis sections and found a 12% decrease in infarct surface area from day 1 to 21 (70). Roberts and colleagues reported a 17% decrease in infarct circumferential segment length from day 2 to 21 using similar methods (225). In dogs, Jugdutt et al. and Richard et al. reported 39% and 30% decreases, respectively, in infarct circumferential segment length over six weeks of healing, measured using computerized planimetry of short-axis sections (122, 223). Reports of scar compaction suggest the existence of one or more remodeling mechanisms that can overcome elevated local stresses due to scar thinning; as discussed under Therapeutic Modification of Scar Structure and Properties below, therapeutic approaches to enhance intrinsic scar compaction are currently under development.

Measures of Post-Infarction Function

Assessing heart function can be particularly challenging following myocardial infarction, because so many things are changing at the same time. Consider the excellent Handbook of Physiology chapter, “Systolic and Diastolic Function (Mechanics) of the Intact Heart,” by Covell and Ross, which is available as legacy content in this Comprehensive Physiology

series (50). Nearly all of the determinants of systolic function discussed in that article change during myocardial infarction and subsequent LV remodeling, including: cardiac shape and dimensions, preload, afterload, contractility (inotropic state), and beta-adrenergic stimulation. Against this complex background of time-varying changes, it is critical to understand what information individual functional measures provide, and how and when their interpretation is most likely to be confounded. In particular, measurements of ejection fraction are frequently used inappropriately in the literature to claim that individual therapies improve LV function, when in fact those therapies alter LV size or hemodynamics *without* improving function. Therefore, before discussing how myocardial scar structure impacts function in the next section, we review here the most commonly used functional measures and discuss their interpretation in the setting of myocardial infarction (Table 1). This section focuses on LV function, which is usually of primary interest in post-infarction studies.

Assessing Diastolic Function Following Infarction

Immediately following a myocardial infarction, the acute drop in LV function triggers a number of compensatory reflexes. One of these reflexes is constriction of the systemic veins, where most of the blood volume typically resides. Venoconstriction shifts blood from the veins into the rest of the circulatory system, thereby increasing pressures. In particular, Burkhoff and Tyberg employed a circuit model of the circulatory system to demonstrate that venoconstriction appears to be primarily responsible for the increases in pulmonary and LV end-diastolic pressures (EDP) observed following a large myocardial infarction (30). Consistent with that model prediction, Goldman and coworkers found that the systemic veins are constricted in rats with post-infarction heart failure, and that vasodilators that act on veins lower LV EDP, while those that selectively lower arterial resistance do not (84, 219). Elevated EDP immediately following an infarction plays an important role in preserving systolic function through the Frank-Starling mechanism, whereby increased diastolic pre-stretch leads to greater systolic force generation in the undamaged myocardium (191). However, severe elevations lead to pulmonary edema and congestive heart failure. The fact that EDP is changing following an infarction is important to keep in mind when interpreting changes in end-diastolic volume (EDV), by far the easiest diastolic parameter to measure noninvasively, and therefore one of the most commonly reported in studies of myocardial infarction. Obviously, if EDP changes, then EDV will change as well, even in the absence of ventricular remodeling or changes in myocardial mechanical properties.

Measuring the relationship between EDP and EDV over a range of loading conditions – the end-diastolic pressure-volume relationship, or EDPVR – provides the clearest picture of how the diastolic properties of the heart are changing. Yet even this relationship must be interpreted with care following myocardial infarction. The EDPVR reflects both the material properties of the myocardium itself and the geometry of the LV. If part of the LV becomes stiffer due to scar formation (see Infarct Material Properties below), then the EDPVR should shift to the left, reflecting the greater pressure required to inflate the ventricle to a given volume. On the other hand, if the LV dilates, the EDPVR should shift to the right. This is because LV dilation occurs through a growth process that increases the circumference of the unloaded ventricle; as a result, at any given volume the myocardium is less stretched than it was prior to remodeling, resulting in lower stresses in the wall and lower pressure in the

cavity. The great challenge of interpreting the EDPVR following infarction is that both of these changes occur simultaneously. The healing scar becomes stiffer, pushing the EDVPR leftward, but the ventricle also dilates, pushing the EDPVR rightward. In rats, Pfeffer et al. found that the balance between these two effects depended on both infarct size and time: with small infarcts, changes in infarct stiffness and LV dilation largely offset one another, producing little overall change in the EDPVR, while with larger infarcts the dilation dominated and the EDPVR shifted progressively rightward (Figure 5) (204). Even relatively simple computational models can separate the effects of infarct stiffness and LV dilation if data on both are available (23, 251); accordingly, such models have played an important role in understanding how individual factors affect post-infarction function. The effects of scar formation on both diastolic and systolic function are discussed in more detail in the section on Mechanical Implications of Collagen Content and Crosslinking below.

Assessing Systolic Function Following Infarction

As the region deprived of blood flow during an acute myocardial infarction stops contracting, the pumping ability of the LV is reduced. However, quantifying the drop in function is surprisingly difficult, particularly in animals with intact hemodynamic reflexes (Table 1). Traditionally, the slope E_{max} (maximal elastance) of the end-systolic pressure-volume relationship (ESPVR) is considered to be a reasonably load-independent measure of LV contractility (50, 248). Drugs that enhance contractility increase E_{max}, and drugs that decrease contractility decrease E_{max}. Yet during acute myocardial infarction in dogs, Sunagawa et al. found that E_{max} changed little, while the volume intercept of the ESPVR (V_0) increased dramatically. In other words, the ESPVR shifted rightward rather than decreasing its slope as expected (Figure 6) (251). In the same paper, the authors constructed a remarkably simple compartmental model that both captured this behavior and explained the underlying mechanics. Their key insight was that acutely ischemic myocardium behaves mechanically like passive myocardium, exhibiting the same exponential stress-strain behavior. They therefore modeled the end-systolic pressure-volume behavior of the acutely infarcted LV by taking a weighted average of the volumes contained in a normally contracting LV (normal compartment) and a passively inflated LV (ischemic compartment) at a range of pressures (Figure 6). When the ischemic compartment was inflated to systolic pressures, it moved up to such a steep part of its pressure-volume curve that its slope was similar to that of the normal ESPVR; thus a weighted average of these two slopes differed little from the baseline E_{max}. By contrast, at end-systolic pressure the infarct compartment contained much more volume than if it had been contracting, explaining the rightward shift in the overall ESPVR.

In vivo, changes in hemodynamic variables such as end-systolic pressure (ESP) and volume (ESV), stroke volume (SV), cardiac output (CO), and ejection fraction (EF) are determined both by the underlying change in pump function reflected by the shifted ESPVR and by reflex hemodynamic compensations that occur in response to infarction. For a detailed review of reflex control of arterial pressure, we recommend the Handbook of Physiology chapter “Baroreflex Control of Systemic Arterial Pressure and Vascular Bed” by Sagawa, which is available as legacy content in this Comprehensive Physiology series (234). Broadly, these reflexes act to maintain systemic arterial pressure, and following infarction

they include arterial vasoconstriction, venous vasoconstriction, and increases in heart rate and contractility of noninfarcted myocardium via activation of the sympathetic nervous system. The magnitudes of the compensations depend heavily on infarct size, and their balance varies by species, but here we outline some general trends that aid interpretation of specific hemodynamic measures, based primarily on studies in conscious animals (220, 258). As noted above, E_{max} normally changes little due to an acute infarct; however, dP/dt_{max} (the maximum rate of systolic pressure generation), another commonly used index of contractility, generally decreases as bulging of the ischemic region during isovolumic contraction slows pressure development. Except in the setting of very large infarcts that trigger acute heart failure, reflex compensations typically restore CO to near normal; heart rate (HR) may increase or remain unchanged, and SV may or may not decrease. ESP is often slightly reduced and ESV is nearly always increased, due to the rightward shift of the ESPVR, but should be interpreted with care if ESP is significantly different from control. Because EDV and EDP typically increase (see Diastolic Function above), EF usually decreases even when SV is unchanged.

It should be clear from the discussion above that no single parameter measured *in vivo* in the presence of intact reflexes can reliably indicate the magnitude of systolic dysfunction associated with an acute infarct (Table 1). Among the measures discussed here, EF has become the most commonly reported, probably because it is relatively easy to measure noninvasively and has a well-established range of normal values in patients and common animal models. Unfortunately, changes in EF are often misleading following infarction because both the numerator (SV) and denominator (EDV) change simultaneously. This is particularly problematic for chronic studies of post-infarction healing, which are further complicated by remodeling in both the infarcted and non-infarcted regions of the LV. In experimental settings where preload can be varied, plotting cardiac output as a function of LV EDP is the most reliable way to gauge changes in function independently from the increases in EDP that frequently accompany infarction. This approach reveals that in the setting of a large compensated MI, the cardiac output curve has shifted down and to the right, reflecting reduced function, and CO is normal primarily because EDP is elevated. Readers familiar with CO curves may rightly object that changes in afterload also affect these curves, but in practice the fact that the baroreflexes hold arterial pressure nearly constant limits the impact of this potential confounder.

Assessing Regional Function Following Infarction

Regional measurements have played an essential role in our understanding of the mechanics of myocardial infarction. In their classic study, Tennant and Wiggers tracked local epicardial motion and showed that shortening of the muscle fibers gradually disappeared and was replaced by systolic lengthening over the first minute following coronary occlusion; restoration of normal blood flow after brief occlusions produced full recovery of contraction (255). Tyberg et al. plotted cavity pressure against regional segment lengths measured in healthy myocardium and found counter-clockwise loops similar to pressure-volume loops, reflecting the positive work performed by the muscle during ejection (264). Following just a few seconds of ischemia, these segments no longer traced out active loops when plotted against pressure; instead, they stretched and recoiled along a single curve reflecting the

passive elastic properties of the myocardium. Early ultrasound imaging provided a similar picture of regional mechanics: during acute ischemia or infarction, the normal inward motion of the heart wall was reduced, absent (akinesis), or even replaced by outward motion (dyskinesis). Consequently, qualitative (108) and quantitative (88) analysis of abnormalities in regional wall motion were introduced as new tools to diagnose myocardial ischemia, and recognition of wall motion abnormalities during stress echocardiography became a common clinical approach to screening for coronary artery disease.

Subsequent studies used implanted radiopaque markers (107, 114, 271) or sonomicrometers (258, 259) to track the regional mechanics of ischemic regions and healing infarcts over time and in multiple dimensions. Most of these studies employed strains computed between end diastole and end systole to measure regional mechanics. Today, ultrasound speckle-tracking, MRI tagging, DENSE MRI, and other similar methods can provide non-invasive imaging of strain, allowing concepts from earlier animal studies to be employed in the clinic. However, the shift from active contraction to passive stretching in the ischemic region has some implications that are important to keep in mind. First, a passive infarct stretches not only during filling but also as pressure rises during isovolumic contraction; once ejection begins, wall stresses begin to drop due to the decrease in chamber size, and the infarct begins to passively recoil. In other words, segment lengths in the infarct are not maximum at ED and not minimum at ES. Furthermore, the amount of stretch during LV filling and recoil during LV emptying depend upon the mechanical properties of the tissue and the hemodynamics of the particular animal model (Figure 7). Accordingly, the traditional approach of measuring strain from end diastole to end systole makes less sense than in actively contracting myocardium, and such strains can be difficult to interpret correctly. The second potential difficulty in interpreting strains from the infarct region is that – like EF – strain is a relative measure, and both the numerator and denominator are typically changing following infarction *in vivo*. Another potential confounding factor is that shortening in remaining viable myocardium can complicate interpretation of strain measurements in the setting of non-transmural ischemia or infarction. Finally, as tissue structure, mechanical properties, stresses, and coupling to surrounding myocardium all evolve over time following infarction, strains can change in surprising ways.

In most animal models, in-plane strains (circumferential and longitudinal) drop to near zero immediately after ligation and remain small throughout the course of healing (Figure 8) (73, 114, 258, 259). In many cases, reported mean strains are small relative to the standard deviation of the measurement, and the reported strains are therefore not significantly different from zero. However, some studies with the resolution to detect small amounts of stretching have reported that the magnitude of stretching remains constant over time, as gradual stiffening of the healing infarct is offset by increased stresses resulting from thinning of the infarct and dilation of the LV (73, 114). By contrast, MRI studies in patients tend to report an early drop in shortening within the ischemic region, followed by a gradual recovery (Figure 8) (22, 136, 148, 228). This discrepancy in reported trends in regional mechanics appears to be due primarily to differences in infarct size and transmural extent rather than to differences in surgical or imaging methods: using sonomicrometers, Theroux et al. found no strain recovery following permanent ligation but substantial recovery in

reperfused dog infarcts (Figure 8A), while very large reperfused infarcts in mice failed to show strain recovery on MRI (Figure 8B). We note here that interpretation of radial strains is often much more difficult following infarction. For example, 3 weeks following infarction in pigs, Holmes et al. found that radial strains measured by implanted markers returned to preinfarction levels despite the persistence of abnormal strains in other directions and histologic evidence of dense, transmural scars (114). In chronic studies, measuring strains in more than one direction can help avoid misinterpretation.

Finally, we note that the presence of an infarct can confound interpretation of measures of regional function in the rest of the heart. While shortening in the non-infarcted myocardium increases following infarction (258), part of this shortening is related to the transfer of blood into the ischemic region during isovolumic contraction; therefore, increased local shortening does not necessarily imply better global function. Furthermore, bulging of the ischemic region during isovolumic contraction and recoil during isovolumic relaxation are mechanically similar to the strain patterns observed in a late-activated region of a dyssynchronous heart (16, 135). Therefore, measures of LV dyssynchrony must be interpreted carefully in the setting of myocardial ischemia or infarction.

Assessing Left Ventricular Remodeling Following Infarction

Survivors of MI face a substantial risk of developing heart failure through a gradual process of LV dilation. As a result, treatments such as angiotension converting enzyme inhibitors (ACEis) that can slow post-infarction LV remodeling are a mainstay of clinical therapy, and methods to monitor the progression of LV remodeling non-invasively are essential. In practice, LV volumes are the most commonly used index of LV remodeling, and ESV has demonstrated the best prognostic value (284). As discussed above for diastolic and systolic function, EDV and ESV depend not only on geometry, mechanical properties, and contractile function but also on pressures; therefore, non-invasive measurements of volumes without corresponding pressures can be difficult to interpret in some situations. ESV offers an advantage over EDV in this respect as well: when following remodeling in a single patient, large changes in systolic pressures that could confound interpretation of ESV should be apparent from standard arterial blood pressure measurements, whereas monitoring changes in LV EDP would require catheterization.

Despite the advances in noninvasive strain measurement discussed under Regional Function above, measuring remodeling on a regional basis requires the ability to identify the same individual points within the heart wall at multiple times over the course of remodeling, and therefore remains practical only in laboratory settings where implantation of markers or sonomicrometers is feasible. Implanted markers are typically used to define individual circumferentially or longitudinally oriented segments and track changes in their length over time, and typically show gradual compaction (reduced segment lengths) within the healing scar and dilation (increased segment lengths) in the remote myocardium (114, 258). Not surprisingly, local measures of segment lengths come with the same caveat as global measures of volume: unless pressures are matched experimentally or measured, changes in pressure can confound interpretation.

Mechanical Implications of Scar Structure

Infarct size, location and geometry vary widely among animal models as well as among individual patients who suffer heart attacks; as reviewed above, collagen content, crosslinking, and organization also vary among models and change over time. Because these structural features determine the mechanical properties of the healing infarct and its mechanical interactions with remaining myocardium, they are critical determinants of pump function, remodeling, and the risk of post-infarction complications ranging from infarct rupture to heart failure. As discussed above, within minutes after coronary artery occlusion the ischemic region becomes passive and non-contractile. Acutely, the mechanical properties of the infarct still resemble those of passive myocardium and diastolic filling remains unaffected (23). However, during systole the infarct stretches and bulges outward when the remaining intact myocardium is contracting. As a result, the mechanical efficiency of the heart as a pump decreases to an extent that depends strongly on infarct size. The extent of functional depression in turn determines the degree of reflex sympathetic activation, which initially preserves LV function but becomes problematic in the long term: prolonged sympathetic activation is associated with progression of chronic heart failure (26, 261). As the scar forms and its collagen structure evolves, changes in infarct mechanical properties interact with geometric remodeling of both the infarct and the noninfarcted regions of the left ventricle to govern changes in diastolic and systolic function, ongoing remodeling, and ultimately clinical prognosis.

Mechanical Implications of Infarct Geometry

Infarct Size—Infarct size is one of the most important determinants of post-MI ventricular function. Larger volumes of ischemic tissue lead to more severe dysfunction during all stages of post-MI healing. In the acute stage after MI, functional depression stems primarily from reduced active contraction during systole, and the degree of systolic impairment is determined by the size of the ischemic area. For example, in the classic study of acute ischemia discussed in the previous section (Figure 6), Sunagawa et al. found that the magnitude of the rightward shift in the ESPVR was linearly proportional to the size of the ischemic region (251). In a porcine model of MI, Savage et al. similarly found that systolic wall thickening decreased with increasing extent of necrosis (236). Clinically, patients with larger infarcts upon admission have lower CO and SV, decreased LV stroke work, and elevated LV filling pressures (171). Infarct size also correlates with changes in function at later time points following infarction: chronic changes in EDP, LV volume, CO, dP/dt_{max}, and systolic arterial pressure all vary in proportion to infarct size several weeks after infarction in the rat (71, 207).

The amount of infarcted tissue is also a critical determinant of post-MI remodeling: larger infarcts not only cause more severe functional depression, but also carry a greater risk of LV dilation. In rats, both increases in LV volume and decreases in infarct thickness over 2-4 weeks post-MI are proportional to infarct size (71, 111). Over several months of remodeling in rats, Pfeffer found monotonic increases in LV volume and LV volume:mass ratio at matched values of LV pressure (LVP) across small, moderate, and large infarct groups (204). In patients, increases in EDV and ESV have also been shown to be positively related

to infarct size over both short (30 days) and long (6-12 months) periods of remodeling (Figure 9), regardless of infarct location (41, 177).

Given their impact on both function and remodeling, it is not surprising that larger infarcts lead to poorer prognoses. In one study, the location of coronary artery ligation was varied to produce a range of infarct sizes in rats. One-year survival monotonically decreased between the sham, small, medium, and large infarct groups, and the most dramatic increase in the relative risk of death was observed between infarcts covering 40-50% of the LV (206). Several clinical studies have established a similar correlation between infarct size and clinical outcome. Studies using PET and gadolinium-enhanced MR imaging to determine infarct size reported increased mortality or decreased event-free survival 2-3 years post-MI in groups with large infarcts (289, 294). In another study, infarct size measured at 3 months post-MI was a stronger predictor of 1.5 year mortality than either LVEF or LV volumes (227). Finally, in an autopsy study of 54 patients, Page and colleagues found that all patients with >40% LV scar had cardiogenic shock, while no patients with <35% scar had shock (199). Interestingly, this study showed that risk is related to the cumulative amount of scar in the ventricle, rather than to the size of the most recent infarct: several small infarcts could lead to the same poor prognosis as a single large infarct, provided that similar volumes of scar are present.

Infarct Location—In addition to infarct size, the location of scar in the ventricle (determined by the affected coronary arteries) also plays an important role in determining function, remodeling, and prognosis following MI. Infarcts on the anterior wall of the LV, arising from occlusion of the left anterior descending coronary artery (LAD), lead to greater functional detriment and worse clinical outcomes than similarly sized infarcts in other locations. Several studies reporting clinical follow-up of patients suffering a first MI have found that anterior infarcts lead to greater risk of chronic heart failure (HF) and mortality (105, 246, 256). Stone et al. reported that patients with large, anterior MIs exhibited HF and cardiac mortality rates more than double those of patients with inferior infarcts (246), and Hands and coworkers reported the same trends after controlling for infarct size (105). Unfortunately, the anterior wall is also the most frequently observed site of infarction (14, 239, 246, 256).

Rupture of the injured myocardium following infarction is a catastrophic event and in an early report accounted for 10-20% of fatalities occurring between 1-21 days post-MI (239). Although studies have reported modulation of rupture risk with infarct location, there are conflicting reports on which location carries the greatest risk. Several reports suggest that anterior infarcts are less likely to rupture than infarcts in other locations, or that risk of septal rupture is lower following anterior rather than inferior MI (181, 239). Other studies have reported that, despite differences in the frequency of infarction, risk of rupture is similar for infarcts on the anterior, posterior, lateral, and septal walls (14, 187).

The location of scar also plays a role in determining the extent of post-MI LV remodeling. Infarct location is correlated with changes in LV volume indices (197) and the degree of infarct expansion, with anterior infarcts exhibiting the greatest expansion likelihood (210). Significant post-MI LV cavity dilation occurs in a higher percentage of first-MI patients

with anterior vs. non-anterior infarction (83, 177). Additionally, the degree of remodeling, quantified by changes in absolute cavity volumes, is more severe in anterior MI patients (177). Since various scar locations have different likelihood of involving papillary muscles or adjacent myocardium, it is possible that differences in remodeling partially stem from differences in the likelihood of ischemic mitral regurgitation (MR) (92). MR following MI is associated with larger LV volumes, higher incidence of HF, and diminished long-term survival (1, 4, 13, 97). However, reported rates of MR in acute MI vary widely, from 3-70%, depending on the characteristics of the patient population, degree of MR reported, detection method used, and timeline of follow-up (17). There are also conflicting reports on whether different infarct locations are associated with increased risk of MR (31). Several clinical studies have reported greater incidence of MR following inferior (89, 149, 151) or anterior infarction (154), while others report no difference (32, 202). Ovine studies of ischemic MR have shown that posterior infarcts of varying size were sufficient to induce MR, while anterior infarcts (even those including the anterior papillary muscle) were not (94, 95). However, in another ovine study, Guy and associates concluded that ischemic MR was a consequence, not a cause, of post-infarction LV remodeling (100).

Transmural Extent—A third parameter that plays a role in determining post-MI clinical outcome is the transmural extent of infarction. However, discerning the relative risk of mortality with a transmural versus non-transmural infarct is partially confounded by differences in the risk of recurrent infarction. While some studies suggest that the transmural extent of scar does not lead to differences in early or late mortality (224), there are more reports of elevated risk of acute mortality or in-hospital death following transmural infarction (117, 125, 190, 253). Non-transmural infarction carries less risk of acute mortality, but patients with a non-transmural MI are more likely to suffer a recurrent MI (169, 170, 190). One study of acute MI patients found that the incidence of recurrent MI following non-transmural infarction was over 5 times greater than following transmural MI (170). As a result, late mortality is often higher in patients whose first MI is nontransmural (35, 190). These differences in early and late mortality with infarcts of varying transmurality can partially offset, leading to minimal differences in cumulative survival (35, 117, 190, 253).

Mechanical Implications of Collagen Content and Crosslinking

Infarct Rupture—As discussed above, the first few days following infarction are characterized by myocyte necrosis and inflammation. Immune cells migrate into the infarct area to remove necrotic myocytes and cellular debris (19). Recruitment and activation of MMPs, which degrade collagen and other components of myocardial ECM, can occur as early as 15 minutes post-MI with peak activation observed 1-2 days later (205, 235, 254). As a result, the infarct is mechanically weakest and most prone to rupture during this time, when degradation of the existing structure is underway but before significant deposition of new collagen has begun. In a study of transgenic mice overexpressing the β_2-adrenergic receptor, it was found that higher pre-MI myocardial collagen content is protective against acute infarct rupture (79). In mice, higher incidence of infarct rupture has been observed in mouse strains with higher densities of inflammatory cells in the infarct region (24). Inhibition of certain MMPs and plasminogen activators can reduce rupture frequency, but

can also lead to incomplete removal of necrotic myocytes and impaired scar formation (19, 109). In mice, TIMP-3 deficient animals had a 4-fold increase in cardiac rupture and 50% decrease in survival after LAD ligation (104).

Infarct Material Properties—As discussed elsewhere in this review, within minutes after the onset of ischemia, myocardium stops contracting and begins stretching and recoiling along a curve that reflects its passive properties. Because collagen is a key determinant of those passive properties, it seems logical that early damage to collagen in the ischemic region could not only increase susceptibility to rupture but also reduce the stiffness of the injured muscle. However, it has proven remarkably difficult to test this hypothesis directly. *In vivo* measurements of pressure-segment length curves (211, 257, 258, 264, 273), two-dimensional strains (107), and three-dimensional strains (271) consistently show a shift to longer segment lengths during ischemia. However, this shift could reflect the fact that systolic stresses are now acting on passive myocardium and stretching it to longer lengths, or could in part reflect a shift in the myocardial stress-strain curve itself. The data from our laboratory presented in Figure 7 illustrate the difficulty of distinguishing between these two possibilities: the example pressure-segment length curves from rat (lower panel) seem consistent with a region operating at higher pressures on the same pressure-segment length curve, but the data from dog seem to suggest the entire curve has shifted rightward. Most studies that have varied EDP over a wide enough range to compare segment lengths or strains at matched pressures have concluded that there is a rightward shift of these curves, such that circumferential and longitudinal dimensions are greater even at matched pressures; for a more detailed review of these studies please see Holmes et al. (112).

Here, we focus on the interpretation of these data with regard to changes in collagen structure and material properties. The key point is that even an increase in dimensions at matched pressures doesn't prove that material properties have changed. The early studies of infarct expansion (280) concluded that there was a rearrangement of myocytes, which could change the unstressed length of a region of the infarct, shifting its stress-strain curve to higher lengths without changing the slope or shape of the curve. Furthermore, the early expansion studies reviewed above and at least one three-dimensional study of regional mechanics (271) found early thinning of the ischemic region, which would increase stresses (and therefore strains or segment lengths) at matched cavity pressures even if material properties remained unchanged. Interestingly, May-Newman et al. studied the effect of coronary perfusion pressure on three-dimensional strains during passive inflation of isolated arrested hearts and found that the loss of perfusion decreased wall thickness significantly (173); the changes in wall thickness they observed were large enough to explain the reported levels of radial thinning during regional ischemia induced by coronary occlusion (112). In theory, excising acutely ischemic tissue and mechanically testing it could provide a more definitive answer to whether material properties are changing. However, mechanical testing of normal passive myocardium is technically difficult due to the need to prevent ischemic contracture of the myocytes; following infarction, this problem is compounded by the gradual onset of edema, which can mask changes in material properties due to collagen degradation (112) and increase the disparity between *in vivo* properties and those measured in dissected (unperfused) specimens.

During the fibrotic phase, the relationship between collagen content and scar material properties appears clearer: scar stiffness in the circumferential and longitudinal directions increases in proportion to the accumulation of collagen fibers oriented in those directions. A number of early studies found that the stiffness of healing infarcts increased with a time-course similar to that reported by others for collagen content, but did not directly correlate collagen content and mechanical properties in individual samples. Theroux et al. reported that the slope of passive pressure-segment length curves measured in healing infarcts in dogs increased from 1 to 3 weeks (258), and Connelly et al. found the stiffness of uniaxially tested tissue strips increased progressively from control to 3 and 15 weeks following infarction (48). In human infarcts obtained at autopsy at times ranging from 3 days to 11 years after myocardial infarction, Parmley et al. came closer to correlating mechanics and collagen content: they fitted exponential functions to stress-strain curves obtained from uniaxial tensile tests and found that samples classified as “fibrotic” at autopsy had the highest stiffness coefficients, followed by samples containing a mix of muscle and fibrotic tissue; samples classified as muscular – obtained within the first week after infarction – had the lowest stiffness coefficients (201).

More recent studies have demonstrated that both collagen content and collagen fiber orientation are critical determinants of the mechanical properties of healing infarct scars. Holmes et al. found that collagen fibers in porcine infarcts were strongly aligned in the circumferential direction 3 weeks after coronary ligation; when they tracked strains in these infarcts during passive inflation of isolated arrested hearts, they saw very little stretch in the circumferential direction but more stretch in the longitudinal direction than in remote, noninfarcted myocardium (113). By contrast, Omens et al. saw significant reductions in both circumferential and longitudinal infarct strains during passive inflation of rat hearts tested 2 weeks after coronary ligation (196). A recent study by Fomovsky and Holmes explained why: the collagen fiber structure in healing rat infarcts is isotropic, with no significant alignment in any direction at 1, 2, 3, or 6 weeks following infarction, and these infarcts are mechanically isotropic when subjected to planar biaxial tensile testing (73). This last study by Fomovsky was also one of the few to directly test for a correlation between collagen content and mechanical properties: the authors reported that the stiffness coefficient describing infarct mechanical properties correlated modestly ($R^2 = 0.42$) but significantly with the square of collagen content. Fomovsky and Holmes also measured crosslinking in their study, and concluded that collagen content was a much more important determinant of mechanics than crosslinking. While few studies are available for comparison, one uniaxial tensile testing study examined 3-week rabbit scars following a range of different reperfusion protocols and concluded that tensile strength of those samples correlated strongly with the level of crosslinking rather than with collagen content (49). Finally, we note that a few studies have suggested that at some later point in the remodeling phase, scar stiffness may begin to drop despite the persistently high collagen content. The most intriguing of these is a planar biaxial testing study on sheep infarcts, which showed a clear drop in scar stiffness in both the circumferential and longitudinal directions at 6 weeks after initial increases at 1 and 2 weeks, despite a progressive increase in collagen content (99).

Pump Function—Perhaps the most surprising thing about the dramatic changes in infarct stiffness that occur during healing due to collagen deposition and crosslinking is that these large changes appear to have very little effect on pump function. Early computational models that simulated the functional impact of changes in infarct material properties over the time-course of healing found an interesting trade-off between the effects of scar stiffening on systolic vs. diastolic function (Figure 10) (23, 121). Simulating acute infarcts as noncontractile regions with material properties identical to passive myocardium predicted normal diastolic behavior (reflected in an unchanged EDPVR) but severely depressed systolic function (rightward shift in the ESPVR), in agreement with experiments. Increasing infarct stiffness in the models improved systolic function as expected, shifting the predicted ESPVR back towards baseline. However, hearts with a stiffer infarct also displayed impaired filling, reflected in a left-shifted EDPVR, and the reduced filling offset the improved ejection, producing little overall change in predicted CO at matched pressures. These early models made a number of simplifications, particularly assuming that scar is mechanically isotropic (having the same properties when stretched in any direction), but recent modeling studies using more sophisticated and better-validated finite-element models reached similar conclusions. Fomovsky et al. found that isotropically stiffening a large anterior infarct in a model of an infarcted dog heart reduced both systolic and diastolic volumes at matched pressures, producing no net benefit in overall pump function (74). Similarly, Dang et al. studied the impact of the stiffness of an isotropic patch used in a surgical reshaping procedure in hearts with anterior infarcts and found that increasing patch stiffness reduced systolic and diastolic volumes at matched pressures, but actually decreased SV – in this setting, stiffer patches impaired filling more than they improved ejection (55). Overall, these computational studies are consistent with the majority of the functional evidence for both global and local infarct reinforcement (see the section “Therapeutic Modification of Scar Structure and Properties”): infarct stiffening can be effective in limiting LV dilation, but isotropic reinforcement is unlikely to directly improve LV pump function (20, 180).

Finite-element models have also been used to explore the relationship between infarct stiffness and wall motion in the LV. It has been shown experimentally that post-MI LV dyssynchrony is associated with increased risk of HF and mortality (2). Finite-element models of acute MI in sheep have shown that infarct stiffening is capable of modulating the amount of post-MI dyskinesis, but extreme infarct stiffening was required to render a dyskinetic infarct region akinetic. In order to eliminate negative radial strains in the passive infarct during ventricular systole, scar stiffnesses ~300 times greater than that of normal myocardium had to be implemented in the models (55, 281). However, given the detrimental effects of excessive infarct stiffening on LV diastolic function outlined above, it is unlikely that such dramatic increases in scar stiffness would translate to improvements in overall pump function.

Mechanical Implications of Collagen Orientation and Alignment

Fomovsky and colleagues recently proposed one idea for finessing the trade-off between systolic and diastolic function (74). Inspired by the fact that some infarct scars are highly anisotropic (113), they tested whether any choice of different material properties in the

circumferential and longitudinal directions could significantly enhance predicted pump function in a finite element model of a dog heart with a large anterior infarct (74). Those simulations suggested that an infarct that is quite stiff in the longitudinal direction but as compliant as passive myocardium in the circumferential direction would produce the best pump function. One way to achieve these infarct properties would be to direct collagen fiber orientation over the course of healing; however, a more practical alternative is to selectively reinforce the infarct in the longitudinal direction. The hypothesis that longitudinal reinforcement would improve pump function was tested directly by ligating the LAD in open-chest anesthetized dogs and reinforcing the resulting acute infarcts with a modified Dacron patch that was inextensible in the longitudinal direction but free to deform in the circumferential direction (72). Comparison of hemodynamics immediately before and after reinforcement revealed that the anisotropic patch dramatically improved pump function, as indicated by an upward shift in the cardiac output curve. Calculating CO values at a matched EDP revealed that anisotropic reinforcement restored half of the deficit in pump function due to acute MI. Pressure-volume analysis showed that the anisotropic patch caused a leftward shift in the ESPVR, indicating enhanced contractile capability, while the EDPVR remained unchanged, signifying minimal change in the passive behavior of the infarct and therefore minimal interference with diastolic filling of the LV. The ability of this anisotropic patch to produce dramatic restoration of systolic function without depression of diastolic filling makes anisotropy a promising avenue for exploration, not only for local reinforcement but possibly in total ventricular restraint as well.

Mechanical Implications of Scar Remodeling

As outlined under Geometric Remodeling: Thinning, Expansion, and Compaction above, thinning of the infarct region has been well documented in rats (70, 225, 279), dogs (122, 123, 223), pigs (114), and sheep (183), and also reported in humans (116). This thinning occurs in left ventricles that are operating at elevated diastolic pressures, and often undergoing progressive dilation. Therefore, LaPlace's Law suggests that wall stresses are elevated globally in the LV, and are even higher in the thinning infarct area. This can lead to the development of a detrimental positive feedback loop during scar remodeling, in which a thin scar experiences high wall stresses that cause the scar to undergo further thinning and expansion, leading to higher wall stresses. However, as noted earlier under Assessing Regional Function Following Infarction, most studies of strains in healing transmural infarcts reveal little change in strain magnitude over time. Using coupled agent-based and FE models of infarct scar remodeling, Rouillard and Holmes found that gradual increases in stress may be offset by the deposition of new collagen in the scar (231). Observed increases in rat scar stiffness due to ongoing collagen deposition were sufficient to keep strains in the infarct nearly constant over the simulation time-course.

Electrical Implications of Scar Structure

Determinants of Normal Electrical Activity

Electrical activation of the ventricles is primarily determined by: 1) myocyte electrophysiology, 2) intercellular connectivity, 3) regional differences of both myocyte electrophysiology and connectivity, and 4) three-dimensional tissue structure. In healthy

ventricular myocardium, the normal balance of these factors ensures the efficient and stable spread of electrical impulses through the tissue (reviewed in (243)). Overall, myocytes are aligned in parallel, in a fiber-like arrangement (with well-defined, transmurally varying directionality) and are laterally reinforced, creating 4 to 6 cells-thick laminar layers of tightly coupled myocytes separated by clefts of connective tissue, across which there is little cell-to-cell connectivity (reviewed in (244)). Current between individual cells in these bundles passes through arrays of gap junctions concentrated within intercalated disks, which are generally arranged at the cell ends, transverse to the myocyte axis (although some individual gap junctions are found along the lateral cell membrane - reviewed in (241)). Combined, this tightly organized arrangement of cell orientation and connectivity results in the well-described three-dimensional electrical anisotropy of ventricular tissue, with electrical activation propagating preferentially along the direction of the myocyte axis, with a somewhat slower rate within muscle layers in the transverse direction and an even slower rate transverse to the layers (with a 4:2:1 ratio of conduction speeds) (33, 115).

Electrical Effects of Structural Changes Post-MI

After MI, effects of electrical remodeling are exacerbated by 3D structural changes, which themselves may provide a substrate for re-entrant ventricular tachyarrhythmias (reviewed in (120)). Activation in the infarcted region is characterized by localized delays and fractionated, low-amplitude extracellular electrograms (81). This is typically attributed to changes in patterns of excitation and conduction due to altered ion channel activity (63) and decreased cellular connectivity (240): in the infarct border-zone, myocytes are electrically connected to approximately half of the normal number of adjacent myocytes, with a three-fold greater decrease in lateral versus end-to-end connections due to reduced intercalated disk expression along the cell margin (161). However, an alternative, purely structural mechanism has been proposed (11), which involves tortuous or ‘zig-zag’ conduction in and around infarcted regions through isolated bundles of surviving myocytes (7–9).

Intra-scar Conduction

The orientation, connectivity, and spacing of surviving myocytes affect the speed and anisotropy of electrical conduction, as does the presence or absence of a layer of spared epicardium (146, 265). Computational studies support the idea that surviving myocyte structure within the infarct may explain reported changes in electrical conduction (214). For example, Maglaveras and coworkers showed that simulating tortuous propagation pathways through an infarct can reproduce experimentally obtained electrograms (164, 165). More recently, computational simulations have shown that a uniform decrease in transverse conductivity, combined with axial conduction slowing across an infarcted region, can cause re-entry (269) and that the presence of strands of viable tissue penetrating and forming channels in electrically inert scar are key to ventricular tachyarrhythmia inducibility (3). Rutherford and coworkers reconstructed rat infarcts and the surrounding borderzone at high resolution (Figure 11A) and used computational simulations to explore the implications of the network of connected surviving myocytes (232). They found stimulus site-dependent uni-directional propagation and rate-dependent activation delays. A component of this delay was caused by tortuous conduction across the scar (Figure 11B) along with regional source-

to-sink mismatch caused by abrupt changes in strand dimensions. Their simulations also predicted conduction block, creating a substrate for re-entrant excitation (Figure 11C).

Heterotypic Cell Coupling

While infarcted tissue is generally thought of as being electrically isolating (10), underscoring the importance of healthy tissue strands for conduction in the infarcted region, recent evidence supports the potential for electrical coupling between fibroblasts and myocytes (reviewed in (141, 142, 229)). *In situ*, fibroblast-myocyte electrical coupling has been demonstrated in the border-zone of isolated mouse hearts using cell-specific expression of voltage-sensitive proteins in fibroblasts (213). Fibroblasts may act as current sinks (locally affecting myocyte excitability, repolarization, and conduction (137, 179)) or serve as short- and long-range conductors between isolated tracts of viable myocytes (82, 96). This heterotypic interaction is enhanced after infarction (268) and may contribute to electrical wave propagation into transmural scars (274). The importance of heterotypic coupling for myocyte electrophysiology has been supported by computational simulations (143). Simulations have also demonstrated the importance of electrical interactions between fibroblasts and strands of surviving myocytes for post-infarction arrhythmogenesis: at intermediate densities, coupled fibroblasts cause action potential shortening and an increase in arrhythmia susceptibility, while at high densities they protect against arrhythmias by causing myocyte depolarization and blocking impulse propagation, and at low densities they have no effect on arrhythmia susceptibility (176). The effects of post-infarction heterotypic coupling may also be exacerbated by non-uniformity of ventricular contraction (215), through mechano-sensitivity of cardiac fibroblasts. Fibroblasts possess a cation non-selective stretch-activated current (245), potentially mediated through transient receptor potential channels (296), such that stretch results in their depolarization (143) and modulation of impulse conduction (262). Fibroblast-mediated stretch-induced changes in myocyte electrophysiology and impulse propagation could contribute to initiation of ventricular tachyarrhythmias during increases in intraventricular volume (34, 37) and may be involved in the elimination of arrhythmias by afterload reduction (64, 184).

Therapeutic Modification of Scar Structure and Properties

Modification of Post-Infarction Inflammation

When considering opportunities to therapeutically modify infarct healing, it is tempting to apply intuition drawn from experience in other tissues. Thus, some authors have identified inflammation or fibrosis as pathologies that should be mitigated following myocardial infarction. Yet this simplistic approach underestimates the potential for unintended consequences, as illustrated dramatically by the example of post-infarction steroid administration. Initial animal studies showed that post-infarction administration of steroids can reduce infarct size, but a clinical trial of post-infarction steroids had to be stopped after steroids induced unexpected increases in infarct size, arrhythmia, and death (226). Follow-up studies in animals showed that a variety of pharmacologic agents that reduce edema and inflammation, including high-dose steroids (101, 167) and non-steroidal anti-inflammatory drugs (27, 102, 103), also aggravate infarct expansion and lead to a thinner scar. More recent studies have shown that macrophage depletion dramatically increases post-infarction

mortality in mice, and that mesenchymal stem cells may influence infarct healing in part by modulating macrophage phenotype (15). It remains unclear how edema and inflammation contribute to infarct material properties and geometric remodeling in the first days after infarction, or how their reduction would cause arrhythmias, but these examples underscore the risks of modifying features of infarct healing before understanding their functional importance.

Modification of Collagen Content

Given the clear importance of collagen content in determining scar mechanical properties, a number of studies have sought to therapeutically modify collagen levels post-MI (Figure 12). Collagen concentration is the balanced result of collagen production and degradation; thus, the most obvious targets for pharmacologic modulation are enzymes related to the synthesis of collagen and those that regulate degradation. On the synthesis side, several groups have inhibited prolyl-4-hydroxylase, achieving an average reduction of 37% in infarct collagen content (67, 193). On the degradation side, Villareal et al. used doxycycline as a broad spectrum MMP inhibitor, but found only a modest increase in collagen content (270); Lindsey and colleagues reported better success with a selective MMP inhibitor that does not affect MMP1, which raised collagen content by 70% (159). Koenig et al. knocked out a variety of MMPs (MMP 2, 8, 9, 13, 14), and achieved roughly a 30% increase in collagen content (140). As an alternate strategy, overexpressing MMP inhibitors has produced mixed results: TIMP2 overexpression produced insignificant change (216), while TIMP1 and TIMP3 knockouts both decreased collagen ~25-30% (52, 104).

In addition to therapies intended to manipulate collagen content, a number of drugs used in patients following infarction may alter collagen content as an unintended side effect. ACEis are widely used in post-infarction patients to slow left ventricular remodeling and the development of heart failure; however angiotensin signaling also plays an important role in regulating fibrosis. Watanabe and colleagues found that the ACEi imidapril resulted in a significant decrease (~45%) of infarct collagen content at 28 days post-MI in a rat model, while the inhibitor ramipril showed a more modest effect (276). Acting on the same signaling pathway, the angiotensin receptor blocker (ARB) candesartan has also been shown to decrease collagen content ~35% in a rat MI model (200). Conversely, β-blockers – another drug typically given to limit LV remodeling and progression to heart failure – were reported to increase collagen content ~60% in 12 week-old rat infarcts (278), while beta-receptor overexpression in mice reduced the increase in infarct collagen ~35% by day 7 post-MI (79). The mechanisms of ACEi, ARB, and β-blocker effects on collagen content are multi-faceted: while affecting intracellular signaling pathways responsible for collagen synthesis, these drugs also have direct and indirect effects on the synthesis and activation of MMPs (160, 238, 267).

Modification of Scar Compaction

As described above in Geometric Remodeling: Thinning, Expansion, and Compaction, many reports show infarct compaction over time in the circumferential-longitudinal plane. This finding suggests an endogenous mechanism responsible for compacting scar tissue, which might be amenable to therapeutic manipulation. One plausible hypothesis is that contractile

myofibroblasts drive scar compaction through active force generation. Supporting this hypothesis, Laeremans et al. and Barandon et al. each modulated the Wnt/Frizzled signaling pathway in mice to increase fibroblast density within infarcts and reported increased scar thickness and decreased scar circumferential length, despite a concurrent decrease in infarct collagen content (12, 150).

Mechanical Unloading

Post-MI remodeling is characterized by infarct thinning and ventricular dilation, both of which are thought to be driven at least in part by increases in mechanical loading following infarction. Accordingly, global and local mechanical unloading have been explored as potential therapies to attenuate both infarct and LV remodeling and improve cardiac function. In many cases, the devices employed in these studies were originally developed for use in end-stage failing hearts. However, the extremely poor prognosis of post-infarction heart failure has motivated a number of investigators to explore the idea of mechanically unloading infarcted hearts early after MI, in order to prevent remodeling before it occurs, rather than treating it after it occurs.

LVADs—Early post-infarction application of left ventricular assist devices (LVADs) has been mostly limited to cases of acute MI complicated by cardiogenic shock. Due to the increased risk of LVAD implantation early after infarction (associated with mortality rates as high as 75%) (43), many current post-MI studies now use percutaneous devices. However, the use of percutaneous LVADs in acute MI patients is primarily as a short term, bridge-to-surgery or bridge-to-recovery therapy (260). A meta-analysis of clinical trial data comparing the TandemHeart and Impella LP2.5 devices revealed that, despite improved coronary index and mean arterial pressure, neither device improved patient mortality compared to intra-aortic balloon pumping (45). Because mechanical unloading reduces wall stresses and oxygen consumption, some investigators have also explored acute unloading as a mechanism for reducing infarct size. Kapur et al. found that TandemHeart support during the reperfusion period in a porcine infarct model led to smaller infarct sizes in the LVAD group, although the observed myocardial salvage did not translate to improvements in SV, CO, or ESP (128). Therefore, although mortality due to cardiogenic shock remains high, more data are needed to determine the best choice for active circulatory assistance and to assess long-term effects of these approaches on remodeling, pump function, and survival.

Global Restraint—As an alternative to mechanical unloading by active support, several passive restraint devices have been used to restrain one or both ventricles in an attempt to modulate post-infarction ventricular remodeling (Table 2). The Acorn Corcap cardiac support device (CSD) is a mesh-like device that surrounds the heart, covering both the left and right ventricles. The knitted polyester device is intended to reduce the degree of stretching and the magnitude of wall stress at ED (198). The Paracor HeartNet CSD is another passive, bi-ventricular restraint device consisting of a wire Nitinol mesh that wraps around both ventricles. A third device, the Myocor Coapsys (Myosplint), applies restraint only to the LV. The Coapsys consists of several pairs of rigid pads placed on opposing surfaces of the LV epicardium (anterior and posterior walls) and connected through the cavity by a tension member. Increasing the tension between the two epicardial pads reshapes

the enlarged LV, creating a bilobular ventricle with decreased chamber radius (174). As detailed in a recent review (46), a consistent theme emerges among studies of bi-ventricular or LV restraint devices: global post-MI restraint reduces LV cavity size and decreases the severity of dilation but fails to generate definitive improvements in LV function (20, 21, 42, 85, 98, 166, 174, 209, 212). A similar trend is also observed with another variation of passive LV restraint: optimized and adjustable restraint. Several studies in sheep have examined the effects of a fluid-filled bladder device, which can be inflated and deflated to achieve an optimum restraint level (87, 153). In a study of optimized, static LV restraint, Ghanta and associates found that the degree of restraint decreased over time as the LV cavity reverse remodeled, to the point where there was no longer any restraint pressure being applied at the conclusion of the experiment (87). A follow-up study by the same group compared optimized static restraint to adjustable restraint, in which fluid was added to the balloon lumen to maintain a constant restraint pressure over the course of remodeling (153). Although adjustable restraint was more effective in limiting LV dilation, no functional improvements were observed compared to the static restraint group.

Local Restraint—In addition to global restraint, local restraint of just the infarct region has been explored for its potential to limit remodeling and improve function (Table 2). Cardiac patches intended for local post-infarction application have taken a variety of forms, from synthetic to cell-seeded to completely tissue engineered. Some aim to mechanically reinforce the infarct, while others are intended primarily to deliver growth factors or cells to the damaged region. Not surprisingly given the diversity of approaches, reports of the effects of local infarct restraint on both ventricular remodeling and function are mixed. While several studies show a decrease in LV volume, diameter, or cross-sectional area with local restraint, there are several other reports in which patch reinforcement fails to reduce dilation, suggesting that it may be more difficult to limit LV dilation with local restraint as opposed to global restraint (40, 78, 90, 91, 134, 158, 180, 208, 242, 301). As with global approaches, studies of local post-infarction restraint have failed to demonstrate conclusive improvements in LV function (133, 158, 180, 301). Similarly, a fluid-filled device for achieving optimized local restraint of only the infarct attenuated increases in LV volumes but did not improve SV, mirroring findings from studies of global adjustable restraint (145).

Polymer Injection

Injection of a variety of materials into the infarct area has also been explored as a potential therapeutic approach (Table 2). Aside from delivery of biological or chemical agents to the non-perfused infarct, injection of materials of varying stiffness can also directly alter scar material properties. Experimental studies employing a variety of animal models have shown that injections into the infarct area reduce the degree of radial infarct thinning and in-plane expansion (54, 186, 218). Several studies reported sustained improvement in functional indices and the degree of remodeling (54, 60, 183, 233), while others suggested that the changes in infarct structure following injection do not prevent post-infarction remodeling (218). Furthermore, one study that observed reduced LV dilation with injection at 4 weeks post-MI found that the degree of dilation in the injection and control groups was similar by 13 weeks (60). Computational approaches have also been used to evaluate the theoretical effects of infarct injection and optimize the distribution of injected material. These models

have shown that the best strategy for reducing wall stress in the infarct is to increase the volume of injected material, although optimization of post-MI SV required more complex injection patterns involving both the infarct and border zone (275, 282). Simulated injection of a calcium hydroxyapatite-based tissue filler into the infarct reduced average ES fiber stress in the scar by 86% (281). Experimentally, however, injecting infarcts with gels of different moduli produced similar functional results: infarcts treated with either an 8kPa or 43kPa hyaluronic hydrogel showed similar changes in infarct wall thickness, LV volumes, EF and CO (118). An extensive summary of materials that have been used in infarct injections, in addition to materials that have been used to construct cardiac patches, can be found in Rane & Christman (217).

Electrical Modification

The most common structural modification for the treatment and prevention of ventricular tachyarrhythmias after MI is the creation of more scar, in order to alter or eliminate potential reentrant circuits. Most often, this is achieved through catheter-based tissue ablation, guided by electrical mapping (in some cases supplemented by structural imaging) to identify the re-entrant isthmus (Figure 13; reviewed in (5, 106)). Ablation of tissue thought to be responsible for aberrant conduction is usually accomplished by delivering radio-frequency energy to the tissue, although cryo-ablation, high-intensity focused ultrasound, lasers, and microwaves are also used. In addition, chemical ablation using ethanol and coil embolization of small coronary arteries has been reported. Another procedure, surgical ventricular reconstruction combined with endocardial resection, is primarily intended to improve LV function, but also offers the benefit of arrhythmia elimination by removing re-entrant pathways (reviewed in (61)).

Novel approaches, aimed at reducing arrhythmia incidence by altering scar structure through biological interventions, are also now emerging. These include strategies that aim to improve impulse propagation or prolong refractoriness (reviewed in (86)). Under these schemes, augmentation of intra-scar conduction is achieved through cardiomyocyte or engineered tissue transplantation (to regenerate the infarct), overexpression of sodium channels (to increase excitability), or methods for improved intercellular coupling (such as engraftment of connexin-expressing cells into the infarcted region). Prolongation of refractoriness, on the other hand, is typically realized by gene therapy targeted at lengthening action potential duration or by cell therapy using engineered cell grafts transfected to express specific potassium channels. An exciting development in the area of post-infarction arrhythmia-substrate modification is the potential for ‘homogenization’ of ventricular scar to improve impulse propagation by bio-enzymatic ablation of arrhythmogenic tissue through topical application of collagenase (290).

Conclusion

Post-infarction healing is a dynamic process. The evolving composition, collagen content and cross-linking, collagen fiber orientation, size, shape, and location of the infarct are important determinants of heart function, remodeling, and prognosis. Understanding the functional implications of specific structural features *in vivo* requires understanding not only

tissue mechanics and heart physiology but also other features of cardiovascular physiology including interactions between the heart and the vasculature and reflex regulation of blood pressure. One important conclusion from the studies reviewed here is that computational modeling is an essential tool for integrating the wealth of information required to understand this complex system. As one example, the fact that restraint devices applied early post-infarction have not improved pump function of the heart may seem surprising, but in fact even early computational models anticipated this result when they demonstrated the trade-off between improved systolic function and impaired diastolic function with increasing infarct stiffness.

A second lesson from the studies reviewed here is that understanding the underlying physiology of post-infarction healing is essential to designing and interpreting experiments. Because pressures, volumes, scar structure and geometry, and reflex compensations are all changing throughout the course of healing, no one parameter provides enough information to judge changes in heart function. This fact has led to many false claims of improved function in polymer injection and stem cell studies where ejection fraction was used as the sole measure of LV function. Moving forward, it is essential that animal studies of post-infarction therapies measure entire pressure-volume relationships or cardiac output curves, or at a minimum compare functional indices at matched pressures. Although manipulation of hemodynamics is often impractical in the clinical setting, clinical studies must also measure pressures whenever possible in order to allow confident interpretation of results.

Finally, looking forward to the potential to devise novel post-infarction therapies, the complexity of scar healing means that a broad array of potential targets are available, and indeed a diverse array of pharmacologic, mechanical, and electrical modifications are under development. On the other hand, the complexity of the system makes predicting effects of therapies particularly challenging, and makes purely experimental optimization of these therapies financially impractical. Here too, computational modeling has an important role to play. As noted above, computational models are increasingly capable of predicting the immediate effects of mechanical interventions, accounting for the known interactions between the infarct, non-infarcted myocardium, and the circulation. Moving forward, multi-scale models that can predict responses to drug-device combinations and computational models that can predict longer-term effects of therapies on scar and ventricular remodeling will be essential to designing and testing post-infarction therapies.

Acknowledgements

The authors acknowledge funding from the National Institutes of Health (R21 HL111546 and R01 HL116449 to JWH), National Science Foundation (NSF/CMMI 1332530 to JWH and NSF Graduate Research Fellowship to SAC), American Heart Association (14POST20460271 to WJR), and the Heart and Stroke Foundation of Canada (to TAQ).

References

1. Amigoni M, Meris A, Thune JJ, Mangalat D, Skali H, Bourgoun M, Warnica JW, Barvik S, Arnold JMO, Velazquez EJ, Van de Werf F, Ghali J, McMurray JJV, Køber L, Pfeffer M, Solomon SD. Mitral regurgitation in myocardial infarction complicated by heart failure, left ventricular dysfunction, or both: prognostic significance and relation to ventricular size and function. Eur Heart J. 2007; 28:326–33. [PubMed: 17251259]

2. Antoni ML, Boden H, Hoogslag GE, Ewe SH, Auger D, Holman ER, van der Wall EE, Schalij MJ, Bax JJ, Delgado V. Prevalence of dyssynchrony and relation with long-term outcome in patients after acute myocardial infarction. Am J Cardiol. 2011; 108:1689–96. [PubMed: 21906706]
3. Arevalo H, Plank G, Helm P, Halperin H, Trayanova N. Tachycardia in post-infarction hearts: insights from 3D image-based ventricular models. PLoS One. 2013; 8:e68872. [PubMed: 23844245]
4. Aronson D, Goldsher N, Zukermann R, Kapeliovich M, Lessick J, Mutlak D, Dabbah S, Markiewicz W, Beyar R, Hammerman H, Reisner S, Agmon Y. Ischemic mitral regurgitation and risk of heart failure after myocardial infarction. Arch Intern Med. 2006; 166:2362–8. [PubMed: 17130390]
5. Arruda M, Fahmy T, Armaganijan L, Di Biase L, Patel D, Natale A. Endocardial and epicardial mapping and catheter ablation of post myocardial infarction ventricular tachycardia: A substrate modification approach. J Interv Card Electrophysiol. 2010; 28:137–45. [PubMed: 20396939]
6. Ashikaga H, Sasano T, Dong J, Zviman MM, Evers R, Hopenfeld B, Castro V, Helm RH, Dickfeld T, Nazarian S, Donahue JK, Berger RD, Calkins H, Abraham MR, Marbán E, Lardo AC, McVeigh ER, Halperin HR. Magnetic resonance-based anatomical analysis of scar-related ventricular tachycardia: implications for catheter ablation. Circ Res. 2007; 101:939–47. [PubMed: 17916777]
7. de Bakker JM, van Capelle FJ, Janse MJ, Tasseron S, Vermeulen JT, de Jonge N, Lahpor JR. Slow conduction in the infarcted human heart. “Zigzag” course of activation. Circulation. 1993; 88:915–26. [PubMed: 8353918]
8. de Bakker JM, van Capelle FJ, Janse MJ, Wilde AA, Coronel R, Becker AE, Dingemans KP, van Hemel NM, Hauer RN. Reentry as a cause of ventricular tachycardia in patients with chronic ischemic heart disease: electrophysiologic and anatomic correlation. Circulation. 1988; 77:589–606. [PubMed: 3342490]
9. de Bakker JM, Coronel R, Tasseron S, Wilde AA, Opthof T, Janse MJ, van Capelle FJ, Becker AE, Jambroes G. Ventricular tachycardia in the infarcted, Langendorffperfused human heart: role of the arrangement of surviving cardiac fibers. J Am Coll Cardiol. 1990; 15:1594–607. [PubMed: 2345240]
10. de Bakker JMT, van Rijen HMV. Continuous and discontinuous propagation in heart muscle. J Cardiovasc Electrophysiol. 2006; 17:567–73. [PubMed: 16684038]
11. de Bakker JMT, van Rijen HVM. Electrocardiographic manifestation of anatomical substrates underlying post-myocardial infarction tachycardias. J Electrocardiol. 2007; 40:S21–5. [PubMed: 17993324]
12. Barandon L, Couffinhal T, Ezan J, Dufourcq P, Costet P, Alzieu P, Leroux L, Moreau C, Dare D, Duplàa C. Reduction of infarct size and prevention of cardiac rupture in transgenic mice overexpressing FrzA. Circulation. 2003; 108:2282–9. [PubMed: 14581414]
13. Barzilai B, Davis VG, Stone PH, Jaffe AS, Group MS. Prognostic significance of mitral regurgitation in acute myocardial infarction. Am J Cardiol. 1990; 65:1169–1175. [PubMed: 2337024]
14. Becker RC, Gore JM, Lambew C, Weaver WD, Rubison RM, French WJ, Tiefenbrunn AJ, Bowlby LJ, Rogers WJ. A composite view of cardiac rupture in the United States National Registry of Myocardial Infarction. J Am Coll Cardiol. 1996; 27:1321–1326. [PubMed: 8626938]
15. Ben-Mordechai T, Holbova R, Landa-Rouben N, Harel-Adar T, Feinberg MS, Abd Elrahman I, Blum G, Epstein FH, Silman Z, Cohen S, Leor J. Macrophage subpopulations are essential for infarct repair with and without stem cell therapy. J Am Coll Cardiol. 2013; 62:1890–1901. [PubMed: 23973704]
16. Bilchick KC, Kuruvilla S, Hamirani YS, Ramachandran R, Clarke SA, Parker KM, Stukenborg GJ, Mason P, Ferguson JD, Moorman JR, Malhotra R, Mangrum JM, Darby AE, Dimarco J, Holmes JW, Salerno M, Kramer CM, Epstein FH. Impact of mechanical activation, scar, and electrical timing on cardiac resynchronization therapy response and clinical outcomes. J Am Coll Cardiol. 2014; 63:1657–66. [PubMed: 24583155]
17. Birnbaum Y, Chamoun AJ, Conti VR, Uretsky BF. Mitral regurgitation following acute myocardial infarction. Coron Artery Dis. 2002; 13:337–44. [PubMed: 12436029]

18. Bishop JE, Greenbaum R, Gibson DG, Yacoub M, Laurent GJ. Enhanced deposition of predominantly type I collagen in myocardial disease. J Mol Cell Cardiol. 1990; 22:1157–65. [PubMed: 2095438]
19. Blankesteijn WM, Creemers E, Lutgens E, Cleutjens JP, Daemen MJ, Smits JF. Dynamics of cardiac wound healing following myocardial infarction: observations in genetically altered mice. Acta Physiol Scand. 2001; 173:75–82. [PubMed: 11678729]
20. Blom AS, Mukherjee R, Pilla JJ, Lowry AS, Yarbrough WM, Mingoia JT, Hendrick JW, Stroud RE, McLean JE, Affuso J, Gorman RC, Gorman JH, Acker M, Spinale FG. Cardiac support device modifies left ventricular geometry and myocardial structure after myocardial infarction. Circulation. 2005; 112:1274–83. [PubMed: 16129812]
21. Blom AS, Pilla JJ, Arkles J, Dougherty L, Ryan LP, Gorman JH, Acker MA, Gorman RC. Ventricular restraint prevents infarct expansion and improves borderzone function after myocardial infarction: a study using magnetic resonance imaging, three-dimensional surface modeling, and myocardial tagging. Ann Thorac Surg. 2007; 84:2004–10. [PubMed: 18036925]
22. Bogaert J, Maes A, Van de Werf F, Bosmans H, Herregods MC, Nuyts J, Desmet W, Mortelmans L, Marchal G, Rademakers FE. Functional recovery of subepicardial myocardial tissue in transmural myocardial infarction after successful reperfusion: an important contribution to the improvement of regional and global left ventricular function. Circulation. 99:36–43. [PubMed: 9884377]
23. Bogen DK, Rabinowitz SA, Needleman A, McMahon TA, Abelmann WH. An analysis of the mechanical disadvantage of myocardial infarction in the canine left ventricle. Circ Res. 1980; 47:728–41. [PubMed: 7418131]
24. van den Borne SWM, van de Schans V a M, Strzelecka AE, Vervoort-Peters HTM, Lijnen PM, Cleutjens JPM, Smits JFM, Daemen MJ a P, Janssen BJ a, Blankesteijn WM. Mouse strain determines the outcome of wound healing after myocardial infarction. Cardiovasc Res. 2009; 84:273–82. [PubMed: 19542177]
25. van den Bos EJ, Mees BME, de Waard MC, de Crom R, Duncker DJ. A novel model of cryoinjury-induced myocardial infarction in the mouse: a comparison with coronary artery ligation. Am J Physiol Heart Circ Physiol. 2005; 289:H1291–300. [PubMed: 15863462]
26. Bristow MR, Ginsburg R, Minobe W, Cubicciotti RS, Sageman S, Lurie K, Billingham ME, Harrison DC, Stinson EB. Decreased catecholamine snsitivity and B-adrenergic-receptor density in failing human hearts. N Engl J Med. 1982; 307:205–211. [PubMed: 6283349]
27. Brown EJ, Kloner RA, Schoen FJ, Hammerman H, Hale S, Braunwald E. Scar thinning due to ibuprofen administration after experimental myocardial infarction. Am J Cardiol. 1983; 51:877–83. [PubMed: 6829446]
28. Brown EJ, Swinford RD, Gadde P, Lillis O. Acute effects of delayed reperfusion on myocardial infarct shape and left ventricular volume: a potential mechanism of additional benefits from thrombolytic therapy. J Am Coll Cardiol. 1991; 17:1641–50. [PubMed: 2033197]
29. Bryant JE, Shamhart PE, Luther DJ, Olson ER, Koshy JC, Costic DJ, Mohile MV, Dockry M, Doane KJ, Meszaros JG. Cardiac myofibroblast differentiation is attenuated by alpha(3) integrin blockade: potential role in post-MI remodeling. J Mol Cell Cardiol. 2009; 46:186–92. [PubMed: 19041328]
30. Burkhoff D, Tyberg JV. Why does pulmonary venous pressure rise after onset of LV dysfunction: a theoretical analysis. Am J Physiol. 1993; 265:H1819–28. [PubMed: 8238596]
31. Bursi F, Enriquez-Sarano M, Jacobsen SJ, Roger VL. Mitral regurgitation after myocardial infarction: a review. Am J Med. 2006; 119:103–12. [PubMed: 16443408]
32. Bursi F, Enriquez-Sarano M, Nkomo VT, Jacobsen SJ, Weston S a, Meverden R a, Roger VL. Heart failure and death after myocardial infarction in the community: the emerging role of mitral regurgitation. Circulation. 2005; 111:295–301. [PubMed: 15655133]
33. Caldwell BJ, Trew ML, Sands GB, Hooks DA, LeGrice IJ, Smaill BH. Three distinct directions of intramural activation reveal nonuniform side-to-side electrical coupling of ventricular myocytes. Circ Arrhythm Electrophysiol. 2009; 2:433–40. [PubMed: 19808500]

34. Calkins H, Maughan WL, Weisman HF, Sugiura S, Sagawa K, Levine JH. Effect of acute volume load on refractoriness and arrhythmia development in isolated, chronically infarcted canine hearts. Circulation. 1989; 79:687–697. [PubMed: 2917392]
35. Cannom DS, Levy W, Cohen LS. The short- and long-term prognosis of patients with transmural and nontransmural myocardial infarction. Am J Med. 1976; 61:452–8. [PubMed: 973641]
36. Cannon RO, Butany JW, McManus BM, Speir E, Kravitz AB, Bolli R, Ferrans VJ. Early degradation of collagen after acute myocardial infarction in the rat. Am J Cardiol. 1983; 52:390–5. [PubMed: 6869292]
37. Cao J, Fu L, Gao Q, Xie R, Qu F. Streptomycin inhibits electrophysiological changes induced by stretching of chronically infarcted rat hearts. J Zhejiang Univ Sci B. 2014; 15:515–21. [PubMed: 24903988]
38. Caorsi V, Toepfer C, Sikkel MB, Lyon AR, MacLeod K, Ferenczi M a. Non-linear optical microscopy sheds light on cardiovascular disease. PLoS One. 2013; 8:e56136. [PubMed: 23409139]
39. Carlyle WC, Jacobson AW, Judd DL, Tian B, Chu C, Hauer KM, Hartman MM, Mcdonald KM. Delayed Reperfusion Alters Matrix Metalloproteinase Activity and Fibronectin mRNA Expression in the Infarct Zone of the Ligated Rat Heart. 1997; 2463:2451–2463.
40. Chachques JC, Trainini JC, Lago N, Cortes-Morichetti M, Schussler O, Carpentier A. Myocardial assistance by grafting a new bioartificial upgraded myocardium (MAGNUM trial): clinical feasibility study. Ann Thorac Surg. 2008; 85:901–8. [PubMed: 18291168]
41. Chareonthaitawee P, Christian TF, Hirose K, Gibbons RJ, Rumberger J a. Relation of initial infarct size to extent of left ventricular remodeling in the year after acute myocardial infarction. J Am Coll Cardiol. 1995; 25:567–73. [PubMed: 7860898]
42. Chaudhry PA, Mishima T, Sharov VG, Hawkins J, Alferness C, Paone G, Sabbah HN. Passive epicardial containment prevents ventricular remodeling in heart failure. Ann Thorac Surg. 2000; 70:1275–1280. [PubMed: 11081885]
43. Chen JM, DeRose JJ, Slater JP, Spanier TB, Dewey TM, Catanese K a, Flannery M a, Oz MC. Improved survival rates support left ventricular assist device implantation early after myocardial infarction. J Am Coll Cardiol. 1999; 33:1903–8. [PubMed: 10362191]
44. Chen X, Nadiarynkh O, Plotnikov S, Campagnola PJ. Second harmonic generation microscopy for quantitative analysis of collagen fibrillar structure. Nat Protoc. 2012; 7:654–69. [PubMed: 22402635]
45. Cheng JM, den Uil C a, Hoeks SE, van der Ent M, Jewbali LSD, van Domburg RT, Serruys PW. Percutaneous left ventricular assist devices vs. intra-aortic balloon pump counterpulsation for treatment of cardiogenic shock: a meta-analysis of controlled trials. Eur Heart J. 2009; 30:2102–8. [PubMed: 19617601]
46. Clarke SA, Ghanta RK, Ailawadi G, Holmes JW. Cardiac Restraint and Support Following Myocardial Infarction. Stud Mechanobiol Tissue Eng Biomater Cardiovasc Card Ther Devices. 2013; 15:169–206.
47. Cleutjens JPM, Kandala JC, Guarda E, Guntaka RV, Weber KT. Regulation of Collagen Degradation in the Rat Myocardium after Infarction. 1995; 1292:1281–1292.
48. Connelly CM, McLaughlin RJ, Vogel WM, Apstein CS. Reversible and irreversible elongation of ischemic, infarcted, and healed myocardium in response to increases in preload and afterload. Circulation. 1991; 84:387–399. [PubMed: 2060109]
49. Connelly CM, Vogel WM, Wiegner a. W, Osmers EL, Bing OH, Kloner R a. Dunn-Lanchantin DM, Franzblau C, Apstein CS. Effects of reperfusion after coronary artery occlusion on post-infarction scar tissue. Circ Res. 1985; 57:562–577. [PubMed: 4042284]
50. Covell JW, Ross J. Systolic and Diastolic Function (Mechanics) of the Intact Heart. Handb Physiol. 2011; 6:741–785.
51. Creemers EEJM, Cleutjens JPM, Smits JFM, Daemen MJ a. P. Matrix Metalloproteinase Inhibition After Myocardial Infarction: A New Approach to Prevent Heart Failure? Circ Res. 2001; 89:201–210. [PubMed: 11485970]
52. Creemers EEJM, Davis JN, Parkhurst AM, Leenders P, Dowdy KB, Hapke E, Hauet AM, Escobar PG, Cleutjens JPM, Smits JFM, Daemen MJAP, Zile MR, Spinale FG. Deficiency of TIMP-1

exacerbates LV remodeling after myocardial infarction in mice. Am J Physiol Heart Circ Physiol. 2003; 284:H364–71. [PubMed: 12388239]

53. Crozatier B, Ross J, Franklin D, Bloor CM, White FC, Tomoike H, McKown DP. Myocardial infarction in the baboon: regional function and the collateral circulation. Am J Physiol. 1978; 235:H413–21. [PubMed: 100019]
54. Dai W, Wold LE, Dow JS, Kloner RA. Thickening of the infarcted wall by collagen injection improves left ventricular function in rats: a novel approach to preserve cardiac function after myocardial infarction. J Am Coll Cardiol. 2005; 46:714–9. [PubMed: 16098441]
55. Dang ABC, Guccione JM, Zhang P, Wallace AW, Gorman RC, Gorman JH, Ratcliffe MB. Effect of ventricular size and patch stiffness in surgical anterior ventricular restoration : a finite element model study. Ann Thorac Surg. 2005; 79:185–193. [PubMed: 15620941]
56. Daskalopoulos EP, Janssen BJA, Blankesteijn WM. Myofibroblasts in the infarct area: concepts and challenges. Microsc Microanal. 2012; 18:35–49. [PubMed: 22214878]
57. Dewald O, Ren G, Duerr GD, Zoerlein M, Klemm C, Gersch C, Tincey S, Michael LH, Entman ML, Frangogiannis NG. Of Mice and Dogs : Species-Specific Differences in the Inflammatory Response Following Myocardial Infarction. Am J Pathol. 2004; 164:665–677. [PubMed: 14742270]
58. Dobaczewski M, Bujak M, Zymek P, Ren G, Entman ML, Frangogiannis NG. Extracellular matrix remodeling in canine and mouse myocardial infarcts. Cell Tissue Res. 2006; 324:475–88. [PubMed: 16496177]
59. Dobaczewski M, Gonzalez-Quesada C, Frangogiannis NG. The extracellular matrix as a modulator of the inflammatory and reparative response following myocardial infarction. J Mol Cell Cardiol. 2010; 48:504–11. [PubMed: 19631653]
60. Dobner S, Bezuidenhout D, Govender P, Zilla P, Davies N. A synthetic non-degradable polyethylene glycol hydrogel retards adverse post-infarct left ventricular remodeling. J Card Fail. 2009; 15:629–36. [PubMed: 19700140]
61. Doenst T, Faerber G, Grandinac S, Kuntze T, Menicanti L, Borger MA, Mohr FW. Surgical therapy of ventricular arrhythmias. Herzschrittmacherther Elektrophysiol. 2007; 18:62–7. [PubMed: 17646937]
62. Doi M, Kusachi S, Murakami T, Ninomiya Y, Murakami M, Nakahama M, Takeda K, Komatsubara I, Naito I, Tsuji T. Time-dependent changes of decorin in the infarct zone after experimentally induced myocardial infarction in rats: comparison with biglycan. Pathol Res Pract. 2000; 196:23–33. [PubMed: 10674269]
63. Dun W, Baba S, Yagi T, Boyden PA. Dynamic remodeling of K+ and Ca2+ currents in cells that survived in the epicardial border zone of canine healed infarcted heart. Am J Physiol Heart Circ Physiol. 2004; 287:H1046–54. [PubMed: 15087289]
64. Durrer JD, Lie KI, van Capelle FJ, Durrer D. Effect of sodium nitroprusside on mortality in acute myocardial infarction. N Engl J Med. 1982; 306:1121–8. [PubMed: 7040955]
65. Eaton LW, Weiss JL, Bulkley BH, Garrison JB, Weisfeldt ML. Regional cardiac dilatation after acute myocardial infarction: recognition by two-dimensional echocardiography. N Engl J Med. 1979; 300:57–62. [PubMed: 758578]
66. Erlebacher JA, Weiss JL, Weisfeldt ML, Bulkley BH. Early dilation of the infarcted segment in acute transmural myocardial infarction: role of infarct expansion in acute left ventricular enlargement. J Am Coll Cardiol. 1984; 4:201–8. [PubMed: 6234343]
67. Fielitz J, Philipp S, Herda LR, Schuch E, Pilz B, Schubert C, Günzler V, Willenbrock R, Regitz-Zagrosek V. Inhibition of prolyl 4-hydroxylase prevents left ventricular remodelling in rats with thoracic aortic banding. Eur J Heart Fail. 2007; 9:336–42. [PubMed: 17145199]
68. Fieno DS, Hillenbrand HB, Rehwald WG, Harris KR, Decker RS, Parker MA, Klocke FJ, Kim RJ, Judd RM. Infarct resorption, compensatory hypertrophy, and differing patterns of ventricular remodeling following myocardial infarctions of varying size. J Am Coll Cardiol. 2004; 43:2124–31. [PubMed: 15172424]
69. Fishbein MC, Maclean D, Maroko PR. The Histopathologic Evolution of Myocardial lnfarction. Chest. 1978; 73:843–849. [PubMed: 657859]

70. Fishbein MC, Maclean D, Maroko PR. Experimental myocardial infarction in the rat: qualitative and quantitative changes during pathologic evolution. Am J Pathol. 1978; 90:57–70. [PubMed: 619696]
71. Fletcher PJ, Pfeffer JM, Pfeffer M a. Braunwald E. Left ventricular diastolic pressure-volume relations in rats with healed myocardial infarction. Effects on systolic function. Circ Res. 1981; 49:618–626. [PubMed: 7261261]
72. Fomovsky GM, Clark SA, Parker KM, Ailawadi G, Holmes JW. Anisotropic reinforcement of acute anteroapical infarcts improves pump function. Circ Heart Fail. 2012; 5:515–22. [PubMed: 22665716]
73. Fomovsky GM, Holmes JW. Evolution of scar structure, mechanics, and ventricular function after myocardial infarction in the rat. Am J Physiol Heart Circ Physiol. 2010; 298:H221–8. [PubMed: 19897714]
74. Fomovsky GM, Macadangdang JR, Ailawadi G, Holmes JW. Model-based design of mechanical therapies for myocardial infarction. J Cardiovasc Transl Res. 2011; 4:82–91. [PubMed: 21088945]
75. Fomovsky GM, Rouillard AD, Holmes JW. Regional mechanics determine collagen fiber structure in healing myocardial infarcts. J Mol Cell Cardiol. 2012; 52:1083–90. [PubMed: 22418281]
76. Frangogiannis NG, Ren G, Dewald O, Zymek P, Haudek S, Koerting A, Winkelmann K, Michael LH, Lawler J, Entman ML. Critical role of endogenous thrombospondin-1 in preventing expansion of healing myocardial infarcts. Circulation. 2005; 111:2935–42. [PubMed: 15927970]
77. Frangogiannis NG. The inflammatory response in myocardial injury, repair, and remodelling. Nat Rev Cardiol. 2014; 11:255–65. [PubMed: 24663091]
78. Fujimoto KL, Tobita K, Merryman WD, Guan J, Momoi N, Stolz DB, Sacks MS, Keller BB, Wagner WR. An elastic, biodegradable cardiac patch induces contractile smooth muscle and improves cardiac remodeling and function in subacute myocardial infarction. J Am Coll Cardiol. 2007; 49:2292–300. [PubMed: 17560295]
79. Gao X-M, Dilley RJ, Samuel CS, Percy E, Fullerton MJ, Dart AM, Du X-J. Lower risk of postinfarct rupture in mouse heart overexpressing beta 2-adrenergic receptors: importance of collagen content. J Cardiovasc Pharmacol. 2002; 40:632–40. [PubMed: 12352327]
80. Gao X-M, White D a. Dart AM, Du X-J. Post-infarct cardiac rupture: Recent insights on pathogenesis and therapeutic interventions. Pharmacol Ther. 2012; 134:156–179. [PubMed: 22260952]
81. Gardner PI, Ursell PC, Fenoglio JJ, Wit AL. Electrophysiologic and anatomic basis for fractionated electrograms recorded from healed myocardial infarcts. Circulation. 1985; 72:596–611. [PubMed: 4017211]
82. Gaudesius G, Miragoli M, Thomas SP, Rohr S. Coupling of cardiac electrical activity over extended distances by fibroblasts of cardiac origin. Circ Res. 2003; 93:421–8. [PubMed: 12893743]
83. Gaudron P, Eilles C, Kugler I, Ertl G. Progressive left ventricular dysfunction and remodeling after myocardial infarction. Potential mechanisms and early predictors. Circulation. 1993; 87:755–763. [PubMed: 8443896]
84. Gay R, Wool S, Paquin M, Goldman S. Total vascular pressure-volume relationship in conscious rats with chronic heart failure. Am J Physiol. 1986; 251:H483–9. [PubMed: 3752263]
85. George I, Cheng Y, Yi G-H, He K-L, Li X, Oz MC, Holmes J, Wang J. Effect of passive cardiac containment on ventricular synchrony and cardiac function in awake dogs. Eur J Cardiothorac Surg. 2007; 31:55–64. [PubMed: 17081764]
86. Gepstein L. Cell and gene therapy strategies for the treatment of postmyocardial infarction ventricular arrhythmias. Ann N Y Acad Sci. 2010; 1188:32–8. [PubMed: 20201883]
87. Ghanta RK, Rangaraj A, Umakanthan R, Lee L, Laurence RG, Fox JA, Bolman RM, Cohn LH, Chen FY. Adjustable, physiological ventricular restraint improves left ventricular mechanics and reduces dilatation in an ovine model of chronic heart failure. Circulation. 2007; 115:1201–10. [PubMed: 17339543]
88. Gillam LD, Hogan RD, Foale R a. Franklin TD, Newell JB, Guyer DE, Weyman a. E. A comparison of quantitative echocardiographic methods for delineating infarct-induced abnormal wall motion. Circulation. 1984; 70:113–22. [PubMed: 6723007]

89. Gillinov, a M.; Wierup, PN.; Blackstone, EH.; Bishay, ES.; Cosgrove, DM.; White, J.; Lytle, BW.; McCarthy, PM. Is repair preferable to replacement for ischemic mitral regurgitation? J Thorac Cardiovasc Surg. 2001; 122:1125–41. [PubMed: 11726887]

90. Giraud M-N, Flueckiger R, Cook S, Ayuni E, Siepe M, Carrel T, Tevaearai H. Long-term evaluation of myoblast seeded patches implanted on infarcted rat hearts. Artif Organs. 2010; 34:E184–92. [PubMed: 20482708]

91. Godier-Furnémont AFG, Martens TP, Koeckert MS, Wan L, Parks J. Composite scaffold provides a cell delivery platform for cardiovascular repair. Proc Natl Acad Sci U S A. 2011; 108:7974–7979. [PubMed: 21508321]

92. Godley RW, Wann LS, Rogers EW, Feigenbaum H, Weyman a. E. Incomplete mitral leaflet closure in patients with papillary muscle dysfunction. Circulation. 1981; 63:565–571. [PubMed: 7460242]

93. Goldsmith EC, Bradshaw AD, Spinale FG. Cellular mechanisms of tissue fibrosis. 2. Contributory pathways leading to myocardial fibrosis: moving beyond collagen expression. Am J Physiol Cell Physiol. 2013; 304:C393–402. [PubMed: 23174564]

94. Gorman JH, Gorman RC, Jackson BM, Hiramatsu Y, Gikakis N, Kelley ST, Sutton MG, Plappert T, Edmunds LH. Distortions of the mitral valve in acute ischemic mitral regurgitation. Ann Thorac Surg. 1997; 64:1026–31. [PubMed: 9354521]

95. Gorman JH, Gorman RC, Plappert T, Jackson BM, Hiramatsu Y, St John-Sutton MG, Edmunds LH. Infarct size and location determine development of mitral regurgitation in the sheep model. J Thorac Cardiovasc Surg. 1998; 115:615–22. [PubMed: 9535449]

96. Goshima K, Tonomura Y. Synchronized beating of embryonic mouse myocardial cells mediated by FL cells in monolayer culture. Exp Cell Res. 1969; 56:387–92. [PubMed: 5387911]

97. Grigioni F, Detaint D, Avierinos J-F, Scott C, Tajik J, Enriquez-Sarano M. Contribution of ischemic mitral regurgitation to congestive heart failure after myocardial infarction. J Am Coll Cardiol. 2005; 45:260–7. [PubMed: 15653025]

98. Guccione JM, Salahieh A, Moonly SM, Kortsmit J, Wallace AW, Ratcliffe MB. Myosplint decreases wall stress without depressing function in the failing heart: a finite element model study. Ann Thorac Surg. 2003; 76:1171–80. discussion 1180. [PubMed: 14530007]

99. Gupta KB, Ratcliffe MB, Fallert MA, Edmunds LH, Bogen DK. Changes in passive mechanical stiffness of myocardial tissue with aneurysm formation. Circulation. 1994; 89:2315–26. [PubMed: 8181158]

100. Guy TS, Moainie SL, Gorman JH, Jackson BM, Plappert T, Enomoto Y, St John-Sutton MG, Edmunds LH, Gorman RC. Prevention of ischemic mitral regurgitation does not influence the outcome of remodeling after posterolateral myocardial infarction. J Am Coll Cardiol. 2004; 43:377–83. [PubMed: 15013117]

101. Hammerman H, Kloner R a. Hale S, Schoen FJ, Braunwald E. Dose-dependent effects of short-term methylprednisolone on myocardial infarct extent, scar formation, and ventricular function. Circulation. 1983; 68:446–52. [PubMed: 6861321]

102. Hammerman H, Kloner R a. Schoen FJ, Brown EJ, Hale S, Braunwald E. Indomethacin-induced scar thinning after experimental myocardial infarction. Circulation. 1983; 67:1290–5. [PubMed: 6851023]

103. Hammerman H, Schoen FJ, Braunwald E, Kloner R a. Drug-induced expansion of infarct: morphologic and functional correlations. Circulation. 1984; 69:611–7. [PubMed: 6692521]

104. Hammoud L, Lu X, Lei M, Feng Q. Deficiency in TIMP-3 increases cardiac rupture and mortality post-myocardial infarction via EGFR signaling: beneficial effects of cetuximab. Basic Res Cardiol. 2011; 106:459–71. [PubMed: 21243368]

105. Hands M, Lloyd B, Robinson J, de Klerk N, Thompson P. Prognostic significance of electrocardiographic site of infarction after correction for enzymatic size of infarction. Circulation. 1986; 73:885–891. [PubMed: 3698233]

106. Haqqani HM, Marchlinski FE. Electrophysiologic substrate underlying postinfarction ventricular tachycardia: characterization and role in catheter ablation. Heart Rhythm. 2009; 6:S70–6. [PubMed: 19631910]

107. Hashima AR, Young AA, McCulloch AD, Waldman LK. Nonhomogeneous analysis of epicardial strain distributions during acute myocardial ischemia in the dog. J Biomech. 1993; 26:19–35. [PubMed: 8423166]
108. Heger JJ, Wann LS, Weyman a. E, Dillon JC, Feigenbaum H. Long-term changes in mitral valve area after successful mitral commissurotomy. Circulation. 1979; 59:443–8. [PubMed: 104802]
109. Heymans S, Luttun a, Nuyens D, Theilmeier G, Creemers E, Moons L, Dyspersin GD, Cleutjens JP, Shipley M, Angellilo a, Levi M, Nübe O, Baker a, Keshet E, Lupu F, Herbert JM, Smits JF, Shapiro SD, Baes M, Borgers M, Collen D, Daemen MJ, Carmeliet P. Inhibition of plasminogen activators or matrix metalloproteinases prevents cardiac rupture but impairs therapeutic angiogenesis and causes cardiac failure. Nat Med. 1999; 5:1135–42. [PubMed: 10502816]
110. Hillenbrand HB, Sandstede J, Störk S, Ramsayer B, Hahn D, Ertl G, Koestler H, Bauer W, Ritter C. Remodeling of the infarct territory in the time course of infarct healing in humans. MAGMA. 2011; 24:277–84. [PubMed: 21671093]
111. Hochman JS, Choo H. Limitation of myocardial infarct expansion by reperfusion independent of myocardial salvage. Circulation. 1987; 75:299–306. [PubMed: 3791612]
112. Holmes JW, Borg TK, Covell JW. Structure and mechanics of healing myocardial infarcts. Annu Rev Biomed Eng. 2005; 7:223–53. [PubMed: 16004571]
113. Holmes JW, Nuñez JA, Covell JW. Functional implications of myocardial scar structure. Am J Physiol. 1997; 272:H2123–30. [PubMed: 9176277]
114. Holmes JW, Yamashita H, Waldman LK, Covell JW. Scar remodeling and transmural deformation after infarction in the pig. Circulation. 1994; 90:411–420. [PubMed: 8026026]
115. Hooks DA, Trew ML, Caldwell BJ, Sands GB, LeGrice IJ, Smaill BH. Laminar arrangement of ventricular myocytes influences electrical behavior of the heart. Circ Res. 2007; 101:e103–12. [PubMed: 17947797]
116. Hutchins GM, Bulkley BH. Infarct expansion versus extension: two different complications of acute myocardial infarction. Am J Cardiol. 1978; 41:1127–32. [PubMed: 665522]
117. Hutter AM, DeSanctis RW, Flynn T, Yeatman LA. Nontransmural Myocardial Infarction : A Comparison of Hospital and Late Clinical Course of Patients With That of Matched Patients With Transmural Anterior and Transmural Inferior Myocardial Infarction. Am J Cardiol. 1981; 48:595–602. [PubMed: 7282542]
118. Ifkovits JL, Tous E, Minakawa M, Morita M, Robb JD, Koomalsingh KJ, Gorman JH, Gorman RC, Burdick J a. Injectable hydrogel properties influence infarct expansion and extent of postinfarction left ventricular remodeling in an ovine model. Proc Natl Acad Sci U S A. 2010; 107:11507–12. [PubMed: 20534527]
119. Imanaka-Yoshida K, Hiroe M, Nishikawa T, Ishiyama S, Shimojo T, Ohta Y, Sakakura T, Yoshida T. Tenascin-C modulates adhesion of cardiomyocytes to extracellular matrix during tissue remodeling after myocardial infarction. Lab Invest. 2001; 81:1015–24. [PubMed: 11454990]
120. Janse MJ, Wit AL. Electrophysiological mechanisms of ventricular arrhythmias resulting from myocardial ischemia and infarction. Physiol Rev. 1989; 69:1049–169. [PubMed: 2678165]
121. Janz RF, Waldron RJ. Predicted effect of chronic apical aneurysms on the passive stiffness of the human left ventricle. Circ Res. 1978; 42:255–263. [PubMed: 620446]
122. Jugdutt BI, Amy RWM. Healing after myocardial infarction in the dog: Changes in infarct hydroxyproline and topography. J Am Coll Cardiol. 1986; 7:91–102. [PubMed: 3941223]
123. Jugdutt BI, Joljart MJ, Khan MI. Rate of collagen deposition during healing and ventricular remodeling after myocardial infarction in rat and dog models. Circulation. 1996; 94:94–101. [PubMed: 8964124]
124. Jugdutt BI, Schwarz-Michorowski BL, Khan MI. Effect of long-term captopril therapy on left ventricular remodeling and function during healing of canine myocardial infarction. J Am Coll Cardiol. 1992; 19:713–721. [PubMed: 1538033]
125. Jugdutt BI, Warnica JW. Intravenous nitroglycerin therapy to limit myocardial infarct size, expansion, and complications. Effect of timing, dosage, and infarct location. Circulation. 1988; 78:906–919. [PubMed: 3139326]

126. Jugdutt BI. Remodeling of the myocardium and potential targets in the collagen degradation and synthesis pathways. Curr Drug Targets Cardiovasc Haematol Disord. 2003; 3:1–30. [PubMed: 12769643]

127. Jugdutt BI. Ventricular remodeling after infarction and the extracellular collagen matrix: when is enough enough? Circulation. 2003; 108:1395–403. [PubMed: 12975244]

128. Kapur NK, Paruchuri V, Urbano-Morales JA, Mackey EE, Daly GH, Qiao X, Pandian N, Perides G, Karas RH. Mechanically unloading the left ventricle before coronary reperfusion reduces left ventricular wall stress and myocardial infarct size. Circulation. 2013; 128:328–36. [PubMed: 23766351]

129. Kashem A, Hassan S, Crabbe DL, Melvin DB, Santamore WP, Chitwood WR. Left ventricular reshaping: Effects on the pressure-volume relationship. J Thorac Cardiovasc Surg. 2003; 125:391–399. [PubMed: 12579110]

130. Kashem A, Santamore WP, Hassan S, Crabbe DL, Margulies KB, Melvin DB. CardioClasp: A New Passive Device to Re-Shape Cardiac Enlargement. ASAIO J (American Soc Artif Intern Organs). 2002; 48:253–259.

131. Kashem A, Santamore WP, Hassan S, Melvin DB, Crabbe DL, Margulies KB, Goldman BI, Llort F, Krieger C, Lesniak J. CardioClasp changes left ventricular shape acutely in enlarged canine heart. Journal of Cardiac Surgery. 2003

132. Kass DA, Maughan WL, Ciuffo A, Graves W, Healy B, Weisfeldt ML. Disproportionate epicardial dilation after transmural infarction of the canine left ventricle: acute and chronic differences. J Am Coll Cardiol. 1988; 11:177–85. [PubMed: 3335694]

133. Kellar RS, Shepherd BR, Larson DF, Naughton GK, Williams SK. Cardiac patch constructed from human fibroblasts attenuates reduction in cardiac function after acute infarct. Tissue Eng. 2006; 11:1678–87. [PubMed: 16411813]

134. Kelley ST, Malekan R, Gorman JHI, Jackson BM, Gorman C, Suzuki Y, Plappert T, Bogen DK, John MGS, Edmunds LH. Restraining infarct expansion preserves left ventricular geometry and function after acute anteroapical infarction. Circulation. 1999; 99:135–142. [PubMed: 9884390]

135. Kerckhoffs RCP, McCulloch AD, Omens JH, Mulligan LJ. Effects of biventricular pacing and scar size in a computational model of the failing heart with left bundle branch block. Med Image Anal. 2009; 13:362–9. [PubMed: 18675578]

136. Kidambi A, Mather AN, Swoboda P, Motwani M, Fairbairn TA, Greenwood JP, Plein S. Relationship between myocardial edema and regional myocardial function after reperfused acute myocardial infarction: an MR imaging study. Radiology. 2013; 267:701–8. [PubMed: 23382292]

137. Kizana E, Ginn SL, Smyth CM, Boyd A, Thomas SP, Allen DG, Ross DL, Alexander IE. Fibroblasts modulate cardiomyocyte excitability: implications for cardiac gene therapy. Gene Ther. 2006; 13:1611–5. [PubMed: 16838030]

138. Klocke R, Tian W, Kuhlmann MT, Nikol S. Surgical animal models of heart failure related to coronary heart disease. Cardiovasc Res. 2007; 74:29–38. [PubMed: 17188668]

139. Knowlton AA, Connelly CM, Romo GM, Mamuya W, Apstein CS, Brecher P. Rapid expression of fibronectin in the rabbit heart after myocardial infarction with and without reperfusion. J Clin Invest. 1992; 89:1060–8. [PubMed: 1556175]

140. Koenig GC, Rowe RG, Day SM, Sabeh F, Atkinson JJ, Cooke KR, Weiss SJ. MT1-MMP–Dependent Remodeling of Cardiac Extracellular Matrix Structure and Function Following Myocardial Infarction. Am J Pathol. 2012; 180:1863–1878. [PubMed: 22464947]

141. Kohl P, Camelliti P. Fibroblast-myocyte connections in the heart. Heart Rhythm. 2012; 9:461–4. [PubMed: 21978963]

142. Kohl P, Gourdie RG. Fibroblast-myocyte electrotonic coupling: does it occur in native cardiac tissue? J Mol Cell Cardiol. 2014; 70:37–46. [PubMed: 24412581]

143. Kohl P, Noble D. Mechanosensitive connective tissue: potential influence on heart rhythm. Cardiovasc Res. 1996; 32:62–8. [PubMed: 8776404]

144. Komatsubara I, Murakami T, Kusachi S, Nakamura K, Hirohata S, Hayashi J, Takemoto S, Suezawa C, Ninomiya Y, Shiratori Y. Spatially and temporally different expression of osteonectin and osteopontin in the infarct zone of experimentally induced myocardial infarction in rats. Cardiovasc Pathol. 2003; 12:186–94. [PubMed: 12826287]

145. Koomalsingh KJ, Witschey WRT, McGarvey JR, Shuto T, Kondo N, Xu C, Jackson BM, Gorman JH, Gorman RC, Pilla JJ. Optimized local infarct restraint improves left ventricular function and limits remodeling. Ann Thorac Surg. 2013; 95:155–62. [PubMed: 23146279]

146. Kottkamp H, Vogt B, Hindricks G, Shenasa M, Haverkamp W, Borggrefe M, Breithardt G. Anisotropic conduction characteristics in ischemia-reperfusion induced chronic myocardial infarction. Basic Res Cardiol. 1994; 89:177–191. [PubMed: 8074641]

147. Kramer CM, Lima JA, Reichek N, Ferrari VA, Llaneras MR, Palmon LC, Yeh IT, Tallant B, Axel L. Regional differences in function within noninfarcted myocardium during left ventricular remodeling. Circulation. 1993; 88:1279–88. [PubMed: 8353890]

148. Kramer CM, Rogers WJ, Theobald TM, Power TP, Geskin G, Reichek N. Dissociation between changes in intramyocardial function and left ventricular volumes in the eight weeks after first anterior myocardial infarction. J Am Coll Cardiol. 1997; 30:1625–32. [PubMed: 9385886]

149. Kumanohoso T, Otsuji Y, Yoshifuku S, Matsukida K, Koriyama C, Kisanuki A, Minagoe S, Levine R a. Tei C. Mechanism of higher incidence of ischemic mitral regurgitation in patients with inferior myocardial infarction: Quantitative analysis of left ventricular and mitral valve geometry in 103 patients with prior myocardial infarction. J Thorac Cardiovasc Surg. 2003; 125:135–143. [PubMed: 12538997]

150. Laeremans H, Hackeng TM, van Zandvoort MAMJ, Thijssen VLJL, Janssen BJA, Ottenheijm HCJ, Smits JFM, Blankesteijn WM. Blocking of frizzled signaling with a homologous peptide fragment of wnt3a/wnt5a reduces infarct expansion and prevents the development of heart failure after myocardial infarction. Circulation. 2011; 124:1626–35. [PubMed: 21931076]

151. Lamas GA, Mitchell GF, Flaker GC, Smith SCJ, Gersh BJ, Basta L, Moye L, Braunwald E, Pfeffer MA. Clinical Significance of mitral regurgitation after acute myocardial infarction. Circulation. 1997; 96:827–833. [PubMed: 9264489]

152. Landa N, Miller L, Feinberg MS, Holbova R, Shachar M, Freeman I, Cohen S, Leor J. Effect of injectable alginate implant on cardiac remodeling and function after recent and old infarcts in rat. Circulation. 2008; 117:1388–96. [PubMed: 18316487]

153. Lee LS, Ghanta RK, Mokashi S a, Coelho-Filho O, Kwong RY, Kwon M, Guan J, Liao R, Chen FY. Optimized ventricular restraint therapy: adjustable restraint is superior to standard restraint in an ovine model of ischemic cardiomyopathy. J Thorac Cardiovasc Surg. 2012; 145:824–31. [PubMed: 22698557]

154. Lehmann KG, Francis CK, Dodge HT. Mitral regurgitation in early myocardial infarction. Incidence, clinical detection, and prognostic implications. TIMI Study Group. Ann Intern Med. 1992; 117:10–7. [PubMed: 1596042]

155. Leor J, Tuvia S, Guetta V, Manczur F, Castel D, Willenz U, Petneházy O, Landa N, Feinberg MS, Konen E, Goitein O, Tsur-Gang O, Shaul M, Klapper L, Cohen S. Intracoronary injection of in situ forming alginate hydrogel reverses left ventricular remodeling after myocardial infarction in Swine. J Am Coll Cardiol. 2009; 54:1014–23. [PubMed: 19729119]

156. Lerman RH, Apstein CS, Kagan HM, Osmers EL, Chichester CO, Vogel WM, Connelly CM, Steffee WP. Myocardial healing and repair after experimental infarction in the rabbit. Circ Res. 1983; 53:378–88. [PubMed: 6136345]

157. Lew WY, Chen ZY, Guth B, Covell JW. Mechanisms of augmented segment shortening in nonischemic areas during acute ischemia of the canine left ventricle. Circ Res. 1985; 56:351–8. [PubMed: 3971509]

158. Liao S-Y, Siu C-W, Liu Y, Zhang Y, Chan W-S, Wu EX, Wu Y, Nicholls JM, Li R a, Benser ME, Rosenberg SP, Park E, Lau C-P, Tse H-F. Attenuation of left ventricular adverse remodeling with epicardial patching after myocardial infarction. J Card Fail. 2010; 16:590–8. [PubMed: 20610235]

159. Lindsey ML, Gannon J, Aikawa M, Schoen FJ, Rabkin E, Lopresti-Morrow L, Crawford J, Black S, Libby P, Mitchell PG, Lee RT. Selective matrix metalloproteinase inhibition reduces left ventricular remodeling but does not inhibit angiogenesis after myocardial infarction. Circulation. 2002; 105:753–758. [PubMed: 11839633]

160. Lindsey ML, Zamilpa R. Temporal and spatial expression of matrix metalloproteinases and tissue inhibitors of metalloproteinases following myocardial infarction. Cardiovasc Ther. 2012; 30:31–41. [PubMed: 20645986]

161. Luke RA, Saffitz JE. Remodeling of ventricular conduction pathways in healed canine infarct border zones. J Clin Invest. 1991; 87:1594–1602. [PubMed: 2022731]
162. Ma S, Yang D, Li D, Tang B, Sun M, Yang Y. Cardiac extracellular matrix tenascin-C deposition during fibronectin degradation. Biochem Biophys Res Commun. 2011; 409:321–7. [PubMed: 21586275]
163. Ma Y, de Castro Brás LE, Toba H, Iyer RP, Hall ME, Winniford MD, Lange R a, Tyagi SC, Lindsey ML. Myofibroblasts and the extracellular matrix network in post-myocardial infarction cardiac remodeling. Pflugers Arch. 2014; 466:1113–27. [PubMed: 24519465]
164. Maglaveras N, de Bakker JM, van Capelle FJ, Pappas C, Janse MJ. Activation delay in healed myocardial infarction: a comparison between model and experiment. Am J Physiol Hear Circ Physiol. 1995; 269:0–9.
165. Maglaveras N, Van Capelle FJ, De Bakker JM. Wave propagation simulation in normal and infarcted myocardium: computational and modelling issues. Med Inform (Lond). 23:105–18. [PubMed: 9667044]
166. Magovern JA, Teekell-Taylor L, Mankad S, Dasika U, McGregor W, Biederman RWW, Yamrozik J, Trumble DR. Effect of a flexible ventricular restraint device on cardiac remodeling after acute myocardial infarction. ASAIO J (American Soc Artif Intern Organs). 2006; 52:196–200.
167. Mannisi JA, Weisman HF, Bush DE, Dudeck P, Healy B. Steroid administration after myocardial infarction promotes early infarct expansion. A study in the rat. J Clin Invest. 1987; 79:1431–9. [PubMed: 3571494]
168. Marijianowski MM, Teeling P, Becker a E. Remodeling after myocardial infarction in humans is not associated with interstitial fibrosis of noninfarcted myocardium. J Am Coll Cardiol. 1997; 30:76–82. [PubMed: 9207624]
169. Marmor, a.; Geltman, EM.; Schechtman, K.; Sobel, BE.; Roberts, R. Recurrent myocardial infarction: clinical predictors and prognostic implications. Circulation. 1982; 66:415–421. [PubMed: 7094248]
170. Marmor A, Sobel BE, Roberts R. Factors Presaging Early Recurrent Myocardial Infarction (“Extension”). Am J Cardiol. 1981; 48:603–610. [PubMed: 7282543]
171. Mathey D, Biefield W, Hanrath P, Effert S. Attempt to quantitate relation between cardiac function and infarct size in acute myocardial infarction. Br Heart J. 1974; 36:271–9. [PubMed: 4824535]
172. Matsui Y, Morimoto J, Uede T. Role of matricellular proteins in cardiac tissue remodeling after myocardial infarction. World J Biol Chem. 2010; 1:69–80. [PubMed: 21540992]
173. May-Newman K, Omens JH, Pavelec RS, McCulloch AD. Three-dimensional transmural mechanical interaction between the coronary vasculature and passive myocardium in the dog. Circ Res. 1994; 74:1166–78. [PubMed: 8187283]
174. McCarthy PM, Takagaki M, Ochiai Y, Young JB, Tabata T, Shiota T, Qin JX, Thomas JD, Mortier TJ, Schroeder RF, Schweich CJ, Fukamachi K. Device-based change in left ventricular shape: a new concept for the treatment of dilated cardiomyopathy. J Thorac Cardiovasc Surg. 2001; 122:482–90. [PubMed: 11547298]
175. McCormick RJ, Musch TI, Bergman BC, Thomas DP. Regional differences in LV collagen accumulation and mature cross-linking after myocardial infarction in rats. Am. J. Physiol.
176. McDowell KS, Arevalo HJ, Maleckar MM, Trayanova NA. Susceptibility to arrhythmia in the infarcted heart depends on myofibroblast density. Biophys J. 2011; 101:1307–1315. [PubMed: 21943411]
177. McKay RG, Pfeffer M a. Pasternak RC, Markis JE, Come PC, Nakao S, Alderman JD, Ferguson JJ, Safian RD, Grossman W. Left ventricular remodeling after myocardial infarction: a corollary to infarct expansion. Circulation. 1986; 74:693–702. [PubMed: 3757183]
178. Mehta PM, Alker KJ, Kloner RA. Functional infarct expansion, left ventricular dilation and isovolumic relaxation time after coronary occlusion: a two-dimensional echocardiographic study. J Am Coll Cardiol. 1988; 11:630–6. [PubMed: 2963853]
179. Miragoli M, Gaudesius G, Rohr S. Electrotonic modulation of cardiac impulse conduction by myofibroblasts. Circ Res. 2006; 98:801–810. [PubMed: 16484613]

180. Moainie SL, Guy TS, Gorman JHI, Plappert T, Jackson BM, St John-Sutton MG, Edmunds LH, Gorman RC. Infarct restraint attenuates remodeling and reduces chronic ischemic mitral regurgitation after postero-lateral infarction. Ann Thorac Surg. 2002; 74:444–9. [PubMed: 12173827]

181. Moore, C a.; Nygaard, TW.; Kaiser, DL.; Cooper, a. a.; Gibson, RS. Postinfarction ventricular septal rupture: the importance of location of infarction and right ventricular function in determining survival. Circulation. 1986; 74:45–55. [PubMed: 3708777]

182. Morishita N, Kusachi S, Yamasaki S, Kondo J, Tsuji T. Sequential changes in laminin and type IV collagen in the infarct zone--immunohistochemical study in rat myocardial infarction. Jpn Circ J. 1996; 60:108–114. [PubMed: 8683853]

183. Morita M, Eckert CE, Matsuzaki K, Noma M, Ryan LP, Burdick JA, Jackson BM, Gorman JH, Sacks MS, Gorman RC. Modification of infarct material properties limits adverse ventricular remodeling. Ann Thorac Surg. 2011; 92:617–24. [PubMed: 21801916]

184. Mukherjee D, Feldman MS, Helfant RH. Nitroprusside therapy. Treatment of hypertensive patients with recurrent resting chest pain, ST-segment elevation, and ventricular arrhythmias. JAMA. 1976; 235:2406–2409. [PubMed: 946646]

185. Mukherjee D, Sen S. Alteration of Collagen Phenotypes in Ischemic Cardiomyopathy. J Clin Invest. 1991; 88:1141–1146. [PubMed: 1918369]

186. Mukherjee R, Zavadzkas JA, Saunders SM, McLean JE, Jeffords LB, Beck C, Stroud RE, Leone AM, Koval CN, Rivers WT, Basu S, Sheehy A, Michal G, Spinale FG. Targeted myocardial microinjections of a biocomposite material reduces infarct expansion in pigs. Ann Thorac Surg. 2008; 86:1268–76. [PubMed: 18805174]

187. Naeim F, De La Maza LM, Robbins SL. Cardiac Rupture during Myocardial Infarction: A Review of 44 Cases. Circulation. 1972; 45:1231–1239. [PubMed: 5032820]

188. Nahrendorf M, Wiesmann F, Hiller KH, Hu K, Waller C, Ruff J, Lanz TE, Neubauer S, Haase A, Ertl G, Bauer WR. Serial cine-magnetic resonance imaging of left ventricular remodeling after myocardial infarction in rats. J Magn Reson Imaging. 2001; 14:547–55. [PubMed: 11747006]

189. Naugle JE, Olson ER, Zhang X, Mase SE, Pilati CF, Maron MB, Folkesson HG, Horne WI, Doane KJ, Meszaros JG. Type VI collagen induces cardiac myofibroblast differentiation: implications for postinfarction remodeling. Am J Physiol Heart Circ Physiol. 2006; 290:H323–30. [PubMed: 16143656]

190. Nicod P, Gilpin E, Dittrich H, Polikar R, Hjalmarson a. Blacky a. R, Henning H, Ross J. Short- and long-term clinical outcome after Q wave and non-Q wave myocardial infarction in a large patient population. Circulation. 1989; 79:528–536. [PubMed: 2645061]

191. Nieminen M, Heikkilä J. Echoventriculography in acute myocardial infarction. III. Clinical correlations and implication of the noninfarcted myocardium. Am J Cardiol. 1976; 38:1–8. [PubMed: 937180]

192. Nishioka T, Onishi K, Shimojo N, Nagano Y, Matsusaka H, Ikeuchi M, Ide T, Tsutsui H, Hiroe M, Yoshida T, Imanaka-Yoshida K. Tenascin-C may aggravate left ventricular remodeling and function after myocardial infarction in mice. Am J Physiol Heart Circ Physiol. 2010; 298:H1072–8. [PubMed: 20081106]

193. Nwogu JI, Geenen D, Bean M, Brenner MC, Huang X, Buttrick PM. Inhibition of Collagen Synthesis With Prolyl 4-Hydroxylase Inhibitor Improves Left Ventricular Function and Alters the Pattern of Left Ventricular Dilatation After Myocardial Infarction. Circulation. 2001; 104:2216–2221. [PubMed: 11684634]

194. Oka T, Xu J, Kaiser RA, Melendez J, Hambleton M, Sargent MA, Lorts A, Brunskill EW, Dorn GW, Conway SJ, Aronow BJ, Robbins J, Molkentin JD. Genetic manipulation of periostin expression reveals a role in cardiac hypertrophy and ventricular remodeling. Circ Res. 2007; 101:313–21. [PubMed: 17569887]

195. Olivetti G, Capasso JM, Sonnenblick EH, Anversa P. Side-to-side slippage of myocytes participates in ventricular wall remodeling acutely after myocardial infarction in rats. Circ Res. 1990; 67:23–34. [PubMed: 2364493]

196. Omens JH, Miller TR, Covell JW. Relationship between passive tissue strain and collagen uncoiling during healing of infarcted myocardium. Cardiovasc Res. 1997; 33:351–8. [PubMed: 9074699]

197. Orn S, Manhenke C, Anand IS, Squire I, Nagel E, Edvardsen T, Dickstein K. Effect of left ventricular scar size, location, and transmurality on left ventricular remodeling with healed myocardial infarction. Am J Cardiol. 2007; 99:1109–14. [PubMed: 17437737]

198. Oz MC, Konertz WF, Kleber FX, Mohr FW, Gummert JF, Ostermeyer J, Lass M, Raman J, Acker M a, Smedira N. Global surgical experience with the Acorn cardiac support device. J Thorac Cardiovasc Surg. 2003; 126:983–991. [PubMed: 14566236]

199. Page DL, Caulfield JB, Kastor JA, DeSanctis RW, Sanders CA. Myocardial changes associated with cardiogenic shock. N Engl J Med. 1971; 285:133–137. [PubMed: 5087702]

200. Palaniyappan A, Uwiera RRE, Idikio H, Jugdutt BI. Comparison of vasopeptidase inhibitor omapatrilat and angiotensin receptor blocker candesartan on extracellular matrix, myeloperoxidase, cytokines, and ventricular remodeling during healing after reperfused myocardial infarction. Mol Cell Biochem. 2009; 321:9–22. [PubMed: 18777087]

201. Parmley WW, Chuck L, Kivowitz C, Matloff JM, Swan HJ. In vitro length-tension relations of human ventricular aneurysms. Relation of stiffness to mechanical disadvantage. Am J Cardiol. 1973; 32:889–94. [PubMed: 4271258]

202. Pellizzon GG, Grines CL, Cox D a, Stuckey T, Tcheng JE, Garcia E, Guagliumi G, Turco M, Lansky AJ, Griffin JJ, Cohen DJ, Aymong E, Mehran R, O'Neill WW, Stone GW. Importance of mitral regurgitation inpatients undergoing percutaneous coronary intervention for acute myocardial infarction: the Controlled Abciximab and Device Investigation to Lower Late Angioplasty Complications (CADILLAC) trial. J Am Coll Cardiol. 2004; 43:1368–74. [PubMed: 15093869]

203. Peterson JT, Li H, Dillon L, Bryant JW. Evolution of matrix metalloprotease and tissue inhibitor expression during heart failure progression in the infarcted rat. Cardiovasc Res. 2000; 46:307–15. [PubMed: 10773235]

204. Pfeffer J, Pfeffer M, Fletcher P, Braunwald E. Progressive ventricular remodeling in rat with myocardial infarction. Am J Physiol Heart Circ Physiol. 1991; 260:H1406–14.

205. Pfeffer, M a.; Braunwald, E. Ventricular remodeling after myocardial infarction. Experimental observations and clinical implications. Circulation. 1990; 81:1161–1172. [PubMed: 2138525]

206. Pfeffer, M a.; Pfeffer, JM.; Steinberg, C.; Finn, P. Survival after an experimental myocardial infarction: beneficial effects of long-term therapy with captopril. Circulation. 1985; 72:406–412. [PubMed: 3891136]

207. Pfeffer M, Pfeffer J, Fishbein M, Fletcher P, Spadaro J, Kloner R, Braunwald E. Myocardial infarct size and ventricular function in rats. Circ Res. 1979; 44:503–512. [PubMed: 428047]

208. Piao H, Kwon J-S, Piao S, Sohn J-H, Lee Y-S, Bae J-W, Hwang K-K, Kim D-W, Jeon O, Kim B-S, Park Y-B, Cho M-C. Effects of cardiac patches engineered with bone marrow-derived mononuclear cells and PGCL scaffolds in a rat myocardial infarction model. Biomaterials. 2007; 28:641–9. [PubMed: 17045333]

209. Pilla JJ, Blom AS, Gorman JHI, Brockman DJ, Affuso J, Parish LM, Sakamoto H, Jackson BM, Acker M a, Gorman RC. Early postinfarction ventricular restraint improves borderzone wall thickening dynamics during remodeling. Ann Thorac Surg. 2005; 80:2257–62. [PubMed: 16305885]

210. Pirolo JS, Hutchins GM, Moore GW. Infarct expansion: Pathologic analysis of 204 patients with a single myocardial infarct. J Am Coll Cardiol. 1986; 7:349–354. [PubMed: 2935567]

211. Pirzada, F a.; Ekong, E a.; Vokonas, PS.; Apstein, CS.; Hood, WB. Experimental myocardial infarction. XIII. Sequential changes in left ventricular pressure-length relationships in the acute phase. Circulation. 1976; 53:970–5. [PubMed: 1269134]

212. Power JM, Raman J, Dornom A, Farish SJ, Burrell LM, Tonkin a M, Buxton B, Alferness C a. Passive ventricular constraint amends the course of heart failure: a study in an ovine model of dilated cardiomyopathy. Cardiovasc Res. 1999; 44:549–55. [PubMed: 10690287]

213. Quinn TA, Camelliti P, Siedlecka U, Poggioli T, Loew LM, Knopfel T, Kohl P. Abstract 11749: Cell-Specific Expression of Voltage-Sensitive Protein Confirms Cardiac Myocyte to Non-

Myocyte Electrotonic Coupling in Healed Murine Infarct Border Tissue. Circulation. 2014; 130:A11749.

214. Quinn TA, Kohl P. Combining wet and dry research: Experience with model development for cardiac mechano-electric structure-function studies. Cardiovasc. Res. 2013; 97:601–611. [PubMed: 23334215]
215. Quinn TA. The importance of non-uniformities in mechano-electric coupling for ventricular arrhythmias. J Interv Card Electrophysiol. 2014; 39:25–35. [PubMed: 24338157]
216. Ramani R, Nilles K, Gibson G, Burkhead B, Mathier M, McNamara D, McTiernan CF. Tissue inhibitor of metalloproteinase-2 gene delivery ameliorates postinfarction cardiac remodeling. Clin Transl Sci. 2011; 4:24–31. [PubMed: 21348952]
217. Rane, A a; Christman, KL. Biomaterials for the treatment of myocardial infarction: a 5-year update. J Am Coll Cardiol. 2011; 58:2615–29. [PubMed: 22152947]
218. Rane, A a; Chuang, JS.; Shah, A.; Hu, DP.; Dalton, ND.; Gu, Y.; Peterson, KL.; Omens, JH.; Christman, KL. Increased infarct wall thickness by a bio-inert material is insufficient to prevent negative left ventricular remodeling after myocardial infarction. PLoS One. 2011; 6:e21571. [PubMed: 21731777]
219. Raya TE, Gay RG, Aguirre M, Goldman S. Importance of venodilatation in prevention of left ventricular dilatation after chronic large myocardial infarction in rats: a comparison of captopril and hydralazine. Circ Res. 1989; 64:330–7. [PubMed: 2643489]
220. Raya TE, Gay RG, Lancaster L, Aguirre M, Moffett C, Goldman S. Serial changes in left ventricular relaxation and chamber stiffness after large myocardial infarction in rats. Circulation. 1988; 77:1424–31. [PubMed: 3370778]
221. Reimer, K a; Vander Heide, RS.; Richard, VJ. Reperfusion in acute myocardial infarction: effect of timing and modulating factors in experimental models. Am J Cardiol. 1993; 72:13G–21G.
222. Reimer KA, Jennings RB. The changing anatomic reference base of evolving myocardial infarction. Underestimation of myocardial collateral blood flow and overestimation of experimental anatomic infarct size due to tissue edema, hemorrhage and acute inflammation. Circulation. 1979; 60:866–76. [PubMed: 476891]
223. Richard V, Murry CE, Reimer KA. Healing of myocardial infarcts in dogs. Effects of late reperfusion. Circulation. 1995; 92:1891–901. [PubMed: 7671374]
224. Rigo P, Murray M, Taylor DR, Weisfeldt ML, Strauss HW, Pitt B. Hemodynamic and prognostic findings in patients with transmural and nontransmural infarction. Circulation. 1975; 51:1064–1070. [PubMed: 1132097]
225. Roberts CS, Maclean D, Maroko P, Kloner RA. Early and late remodeling of the left ventricle after acute myocardial infarction. Am J Cardiol. 1984; 54:407–10. [PubMed: 6235736]
226. Roberts R, DeMello V, Sobel BE. Deleterious effects of methylprednisolone in patients with myocardial infarction. Circulation. 1976; 53:I204–6. [PubMed: 1253361]
227. Roes SD, Kelle S, Kaandorp T a M, Kokocinski T, Poldermans D, Lamb HJ, Boersma E, van der Wall EE, Fleck E, de Roos A, Nagel E, Bax JJ. Comparison of myocardial infarct size assessed with contrast-enhanced magnetic resonance imaging and left ventricular function and volumes to predict mortality in patients with healed myocardial infarction. Am J Cardiol. 2007; 100:930–6. [PubMed: 17826372]
228. Rogers WJ, Kramer CM, Geskin G, Hu YL, Theobald TM, Vido DA, Petruolo S, Reichek N. Early contrast-enhanced MRI predicts late functional recovery after reperfused myocardial infarction. Circulation. 1999; 99:744–50. [PubMed: 9989958]
229. Rohr S. Arrhythmogenic implications of fibroblast-myocyte interactions. Circ Arrhythm Electrophysiol. 2012; 5:442–52. [PubMed: 22511661]
230. Rouillard AD, Holmes JW. Mechanical regulation of fibroblast migration and collagen remodelling in healing myocardial infarcts. J Physiol. 2012; 590:4585–602. [PubMed: 22495588]
231. Rouillard AD, Holmes JW. Coupled agent-based and finite-element models for predicting scar structure following myocardial infarction. Prog. Biophys. Mol. Biol. Jul 8.2014 10.1016/j.pbiomolbio.2014.06.010

232. Rutherford SL, Trew ML, Sands GB, Legrice IJ, Smaill BH. High-resolution 3-dimensional reconstruction of the infarct border zone: impact of structural remodeling on electrical activation. Circ Res. 2012; 111:301–11. [PubMed: 22715470]

233. Ryan LP, Matsuzaki K, Noma M, Jackson BM, Eperjesi TJ, Plappert TJ, St John-Sutton MG, Gorman JH, Gorman RC. Dermal filler injection: a novel approach for limiting infarct expansion. Ann Thorac Surg. 2009; 87:148–55. [PubMed: 19101288]

234. Sagawa K. Baroreflex control of systemic arterial pressure and vascular bed. Handb Physiol. 2011; 8:453–496.

235. Sato S, Ashraf M, Millard RW, Fujiwara H, Schwartz a. Connective tissue changes in early ischemia of porcine myocardium: an ultrastructural study. J Mol Cell Cardiol. 1983; 15:261–75. [PubMed: 6876183]

236. Savage RM, Guth B, White FC, Hagan a. D, Bloor CM. Correlation of regional myocardial blood flow and function with myocardial infarct size during acute myocardial ischemia in the conscious pig. Circulation. 1981; 64:699–707. [PubMed: 7273370]

237. Schellings MWM, Vanhoutte D, Swinnen M, Cleutjens JP, Debets J, van Leeuwen REW, d'Hooge J, Van de Werf F, Carmeliet P, Pinto YM, Sage EH, Heymans S. Absence of SPARC results in increased cardiac rupture and dysfunction after acute myocardial infarction. J Exp Med. 2009; 206:113–23. [PubMed: 19103879]

238. Schorb W, Ertl G. Angiotensin II Type 1 receptor induced signal-transduction pathways as new targets for pharmacological treatment of the renin-angiotensin system. Basic Res Cardiol. 1996; 91:91–96. [PubMed: 8957551]

239. Schuster EH, Bulkley BH. Expansion of transmural myocardial infarction: a pathophysiologic factor in cardiac rupture. Circulation. 1979; 60:1532–1538. [PubMed: 498481]

240. Severs NJ, Bruce AF, Dupont E, Rothery S. Remodelling of gap junctions and connexin expression in diseased myocardium. Cardiovasc. Res. 2008; 80:9–19. [PubMed: 18519446]

241. Severs NJ, Coppen SR, Dupont E, Yeh H-I, Ko Y-S, Matsushita T. Gap junction alterations in human cardiac disease. Cardiovasc Res. 2004; 62:368–377. [PubMed: 15094356]

242. Simpson D, Liu H, Fan T-HM, Nerem R, Dudley SC. A tissue engineering approach to progenitor cell delivery results in significant cell engraftment and improved myocardial remodeling. Stem Cells. 2007; 25:2350–7. [PubMed: 17525236]

243. Smaill BH, Zhao J, Trew ML. Three-dimensional impulse propagation in myocardium: Arrhythmogenic mechanisms at the tissue level. Circ. Res. 2013; 112:834–848. [PubMed: 23449546]

244. Spotnitz HM. Macro design, structure, and mechanics of the left ventricle. J Thorac Cardiovasc Surg. 2000; 119:1053–77. [PubMed: 10788831]

245. Stockbridge LL, French AS. Stretch-activated cation channels in human fibroblasts. Biophys J. 1988; 54:187–190. [PubMed: 2458140]

246. Stone PH, Raabe DS, Jaffe AS. Prognostic significance of location and type of myocardial infarction: independent adverse outcome associated with anterior location. J Am Coll Cardiol. 1988; 11:453–463. [PubMed: 3278032]

247. Strungs EG, Ongstad EL, O'Quinn MP, Palatinus JA, Jourdan LJ, Gourdie RG. Cryoinjury Models of the Adult and Neonatal Mouse Heart for Studies of Scarring and Regeneration. Mehods Mol Biol. 2013; 1037:343–353.

248. Suga H, Sagawa K, Shoukas AA. Load independence of the instantaneous pressure-volume ratio of the canine left ventricle and effects of epinephrine and heart rate on the ratio. Circ Res. 1973; 32:314–22. [PubMed: 4691336]

249. Sun Y, Weber KT. Infarct scar: a dynamic tissue. Cardiovasc Res. 2000; 46:250–6. [PubMed: 10773228]

250. Sun Y, Zhang JQ, Zhang J, Lamparter S. Cardiac remodeling by fibrous tissue after infarction in rats. J Lab Clin Med. 2000; 135:316–23. [PubMed: 10779047]

251. Sunagawa K, Maughan WL, Sagawa K. Effect of regional ischemia on the left ventricular end-systolic pressure-volume relationship of isolated canine hearts. Circ Res. 1983; 52:170–8. [PubMed: 6825214]

252. Swift J, Ivanovska IL, Buxboim A, Harada T, Dingal PCDP, Pinter J, Pajerowski JD, Spinler KR, Shin J-W, Tewari M, Rehfeldt F, Speicher DW, Discher DE. Nuclear lamin-A scales with tissue stiffness and enhances matrix-directed differentiation. Science. 2013; 341:1240104. [PubMed: 23990565]

253. Szklo M, Goldberg R, Kennedy HL, Tonascia J a. Survival of patients with nontransmural myocardial infarction: a population-based study. Am J Cardiol. 1978; 42:648–52. [PubMed: 696647]

254. Takahashi S, Barry AC, Factor SM. Collagen degradation in ischaemic rat hearts. Biochem J. 1990; 265:233–241. [PubMed: 2154182]

255. Tennant R, Wiggers CJ. The effect of coronary occlusion on myocardial contraction. Am J Physiol. 1935; 112:351–361.

256. Thanavaro S, Kleiger RE, Province M a, Hubert JW, Miller JP, Krone RJ, Oliver GC. Effect of infarct location on the in-hospital prognosis of patients with first transmural myocardial infarction. Circulation. 1982; 66:742–7. [PubMed: 7116591]

257. Theroux P, Franklin D, Ross J, Kemper WS. Regional myocardial function during acute coronary artery occlusion and its modification by pharmacologic agents in the dog. Circ Res. 1974; 35:896–908. [PubMed: 4214626]

258. Theroux P, Ross J, Franklin D, Covell JW, Bloor CM, Sasayama S. Regional myocardial function and dimensions early and late after myocardial infarction in the unanesthetized dog. Circ Res. 1977; 40:158–165. [PubMed: 844142]

259. Theroux P, Ross J, Franklin D, Kemper WS, Sasayama S. Coronary arterial reperfusion. III. Early and late effects on regional myocardial function and dimensions in conscious dogs. Am J Cardiol. 1976; 38:599–606. [PubMed: 983957]

260. Thiele H, Smalling RW, Schuler GC. Percutaneous left ventricular assist devices in acute myocardial infarction complicated by cardiogenic shock. Eur Heart J. 2007; 28:2057–63. [PubMed: 17586541]

261. Thomas JA, Marks BH. Plasma norepinephrine in congestive heart failure. Am J Cardiol. 1978; 41:233–43. [PubMed: 203177]

262. Thompson SA, Copeland CR, Reich DH, Tung L. Mechanical coupling between myofibroblasts and cardiomyocytes slows electric conduction in fibrotic cell monolayers. Circulation. 2011; 123:2083–2093. [PubMed: 21537003]

263. Trueblood NA, Xie Z, Communal C, Sam F, Ngoy S, Liaw L, Jenkins AW, Wang J, Sawyer DB, Bing OH, Apstein CS, Colucci WS, Singh K. Exaggerated left ventricular dilation and reduced collagen deposition after myocardial infarction in mice lacking osteopontin. Circ Res. 2001; 88:1080–7. [PubMed: 11375279]

264. Tyberg JV, Forrester JS, Wyatt HL, Goldner SJ, Parmley WW, Swan HJC. An Analysis of Segmental Ischemic Dysfunction Utilizing the Pressure-Length Loop. Circulation. 1974; 49:748–754. [PubMed: 4817712]

265. Ursell PC, Gardner PI, Albala A, Fenoglio JJ, Wit AL. Structural and electrophysiological changes in the epicardial border zone of canine myocardial infarcts during infarct healing. Circ Res. 1985; 56:436–451. [PubMed: 3971515]

266. Vandervelde S, Amerongen MJ, Van, Tio RA, Petersen AH, Luyn MJA, Van, Harmsen MC. Increased inflammatory response and neovascularization in reperfused vs . nonreperfused murine myocardial infarction. 2006; 15:83–90.

267. Vanhoutte D, Schellings M, Pinto Y, Heymans S. Relevance of matrix metalloproteinases and their inhibitors after myocardial infarction: a temporal and spatial window. Cardiovasc Res. 2006; 69:604–13. [PubMed: 16360129]

268. Vasquez C, Mohandas P, Louie KL, Benamer N, Bapat AC, Morley GE. Enhanced fibroblast-myocyte interactions in response to cardiac injury. Circ Res. 2010; 107:1011–1020. [PubMed: 20705922]

269. Vigmond E, Vadakkumpadan F, Gurev V, Arevalo H, Deo M, Plank G, Trayanova N. Towards predictive modelling of the electrophysiology of the heart. Exp Physiol. 2009; 94:563–577. [PubMed: 19270037]

270. Villarreal FJ, Griffin M, Omens J, Dillmann W, Nguyen J, Covell J. Early short-term treatment with doxycycline modulates postinfarction left ventricular remodeling. Circulation. 2003; 108:1487–92. [PubMed: 12952845]
271. Villarreal FJ, Lew WY, Waldman LK, Covell JW. Transmural myocardial deformation in the ischemic canine left ventricle. Circ Res. 1991; 68:368–381. [PubMed: 1991344]
272. Vivaldi MT, Eyre DR, Kloner R a, Schoen FJ. Effects of methylprednisolone on collagen biosynthesis in healing acute myocardial infarction. Am J Cardiol. 1987; 60:424–5. [PubMed: 3618516]
273. Vokonas PS, Pirzada F, Hood WB. Experimental myocardial infarction: XII. Dynamic changes in segmental mechanical behavior of infarcted and non-infarcted myocardium. Am J Cardiol. 1976; 37:853–9. [PubMed: 1266750]
274. Walker NL, Burton FL, Kettlewell S, Smith GL, Cobbe SM. Mapping of epicardial activation in a rabbit model of chronic myocardial infarction: J Cardiovasc Electrophysiol. 2007; 18:862–868. [PubMed: 17537208]
275. Wall ST, Walker JC, Healy KE, Ratcliffe MB, Guccione JM. Theoretical impact of the injection of material into the myocardium: a finite element model simulation. Circulation. 2006; 114:2627–35. [PubMed: 17130342]
276. Watanabe R, Ogawa M, Suzuki J-I, Hirata Y, Nagai R, Isobe M. A comparison between imidapril and ramipril on attenuation of ventricular remodeling after myocardial infarction. J Cardiovasc Pharmacol. 2012; 59:323–30. [PubMed: 22130106]
277. Wei S, Chow LT, Shum IO, Qin L, Sanderson JE. Left and right ventricular collagen type I/III ratios and remodeling post-myocardial infarction. J Card Fail. 1999; 5:117–26. [PubMed: 10404351]
278. Wei S, Chow LT, Sanderson JE. Effect of carvedilol in comparison with metoprolol on myocardial collagen postinfarction. J Am Coll Cardiol. 2000; 36:276–281. [PubMed: 10898446]
279. Weisman HF, Bush DE, Mannisi JA, Bulkley BH. Global cardiac remodeling after acute myocardial infarction: a study in the rat model. J Am Coll Cardiol. 1985; 5:1355–62. [PubMed: 3158687]
280. Weisman HF, Bush DE, Mannisi JA, Weisfeldt ML, Healy B. Cellular mechanisms of myocardial infarct expansion. Circulation. 1988; 78:186–201. [PubMed: 2968197]
281. Wenk JF, Eslami P, Zhang Z, Xu C, Kuhl E, Gorman JH, Robb JD, Ratcliffe MB, Gorman RC, Guccione JM. A novel method for quantifying the in-vivo mechanical effect of material injected into a myocardial infarction. Ann Thorac Surg. 2011; 92:935–41. [PubMed: 21871280]
282. Wenk JF, Wall ST, Peterson RC, Helgerson SL, Sabbah HN, Burger M, Stander N, Ratcliffe MB, Guccione JM. A method for automatically optimizing medical devices for treating heart failure: designing polymeric injection patterns. J Biomech Eng. 2009; 131:121011. [PubMed: 20524734]
283. Westermann D, Mersmann J, Melchior A, Freudenberger T, Petrik C, Schaefer L, Lüllmann-Rauch R, Lettau O, Jacoby C, Schrader J, Brand-Herrmann S-M, Young MF, Schultheiss HP, Levkau B, Baba HA, Unger T, Zacharowski K, Tschöpe C, Fischer JW. Biglycan is required for adaptive remodeling after myocardial infarction. Circulation. 2008; 117:1269–76. [PubMed: 18299507]
284. White HD, Norris RM, Brown M a. Brandt PW, Whitlock RM, Wild CJ. Left ventricular end-systolic volume as the major determinant of survival after recovery from myocardial infarction. Circulation. 1987; 76:44–51. [PubMed: 3594774]
285. White M, Rouleau JL, Hall C, Arnold M, Harel F, Sirois P, Greaves S, Solomon S, Ajani U, Glynn R, Hennekens C, Pfeffer M. Changes in vasoconstrictive hormones, natriuretic peptides, and left ventricular remodeling soon after anterior myocardial infarction. Am Heart J. 2001; 142:1056–64. [PubMed: 11717612]
286. Whittaker P, Boughner DR, Kloner RA. Role of collagen in acute myocardial infarct expansion. Circulation. 1991; 84:2123–34. [PubMed: 1934383]
287. Whittaker P, Kloner RA, Boughner DR, Pickering JG. Quantitative assessment of myocardial collagen with picrosirius red staining and circularly polarized light. Basic Res Cardiol. 1994; 89:397–410. [PubMed: 7535519]

288. Whittaker P. Collagen organization in wound healing after myocardial injury. Basic Res Cardiol. 1998; 93(Suppl 3):23–5. [PubMed: 9879440]

289. Wu KC, Zerhouni E a. Judd RM, Lugo-Olivieri CH, Barouch L a. Schulman SP, Blumenthal RS, Lima J a. C. Prognostic Significance of Microvascular Obstruction by Magnetic Resonance Imaging in Patients With Acute Myocardial Infarction. Circulation. 1998; 97:765–772. [PubMed: 9498540]

290. Yagishita D, Ajijola OA, Vaseghi M, Nsair A, Zhou W, Yamakawa K, Tung R, Mahajan A, Shivkumar K. Electrical homogenization of ventricular scar by application of collagenase: A novel strategy for arrhythmia therapy. Circ Arrhythmia Electrophysiol. 2013; 6:776–783.

291. Yamamoto K, Kusachi S, Ninomiya Y, Murakami M, Doi M, Takeda K, Shinji T, Higashi T, Koide N, Tsuji T. Increase in the expression of biglycan mRNA expression Co-localized closely with that of type I collagen mRNA in the infarct zone after experimentally-induced myocardial infarction in rats. J Mol Cell Cardiol. 1998; 30:1749–56. [PubMed: 9769230]

292. Yamanishi A, Kusachi S, Nakahama M, Ninomiya Y, Watanabe T, Kumashiro H, Nunoyama H, Kondo J, Naito I, Tsuji T. Sequential changes in the localization of the type IV collagen alpha chain in the infarct zone: immunohistochemical study of experimental myocardial infarction in the rat. Pathol Res Pract. 1998; 194:413–22. [PubMed: 9689650]

293. Yang F, Liu Y, Yang X, Xu J, Kapke A, Carretero OA. Myocardial infarction and cardiac remodelling in mice. Exp Physiol. 2002; 87:547–555. [PubMed: 12481929]

294. Yoshida K, Gould KL. Quantitative relation of myocardial infarct size and myocardial viability by positron emission tomography to left ventricular ejection fraction and 3-year mortality with and without revascularization. J Am Coll Cardiol. 1993; 22:984–97. [PubMed: 8409073]

295. Young AA, French BA, Yang Z, Cowan BR, Gilson WD, Berr SS, Kramer CM, Epstein FH. Reperfused myocardial infarction in mice: 3D mapping of late gadolinium enhancement and strain. J Cardiovasc Magn Reson. 2006; 8:685–92. [PubMed: 16891227]

296. Yue Z, Zhang Y, Xie J, Jiang J, Yue L. Transient receptor potential (TRP) channels and cardiac fibrosis. Curr Top Med Chem. 2013; 13:270–82. [PubMed: 23432060]

297. Zamilpa R, Lindsey ML. Extracellular matrix turnover and signaling during cardiac remodeling following MI: causes and consequences. J Mol Cell Cardiol. 2010; 48:558–63. [PubMed: 19559709]

298. Zar, JH. Biostatistical Analysis. Pearson Prentice Hall; New Jersey: 2010.

299. Zhou X, Yun J-L, Han Z-Q, Gao F, Li H, Jiang T-M, Li Y-M. Postinfarction healing dynamics in the mechanically unloaded rat left ventricle. Am J Physiol Heart Circ Physiol. 2011; 300:H1863–74. [PubMed: 21398590]

300. Zimmerman SD, Thomas DP, Velleman SG, Li X, Hansen TR, McCormick RJ. Time course of collagen and decorin changes in rat cardiac and skeletal muscle post-MI. Am J Physiol Heart Circ Physiol. 2001; 281:H1816–22. [PubMed: 11557576]

301. Zimmermann W-H, Melnychenko I, Wasmeier G, Didié M, Naito H, Nixdorff U, Hess A, Budinsky L, Brune K, Michaelis B, Dhein S, Schwoerer A, Ehmke H, Eschenhagen T. Engineered heart tissue grafts improve systolic and diastolic function in infarcted rat hearts. Nat Med. 2006; 12:452–8. [PubMed: 16582915]

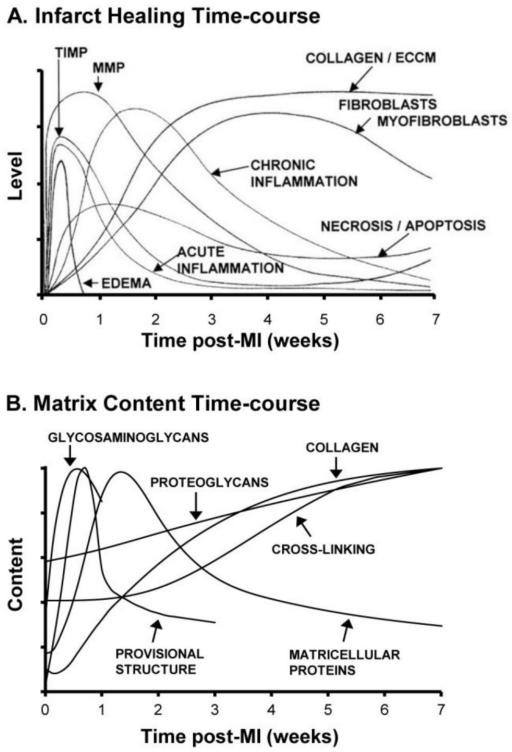

Figure 1.

Wound healing after a myocardial infarction is a multi-faceted, dynamic process that results in the replacement of necrotic myocytes with collagenous scar tissue. **A.** This process is generally divided into 1) an early inflammatory phase characterized by pronounced chemical signaling, resorption of necrotic tissue, and recruitment of myofibroblasts, 2) a fibrotic phase characterized by increased myofibroblast number and collagen accumulation, and 3) a long-term remodeling phase characterized by collagen matrix stabilization and maturation. Panel A. adapted with permission from Jugdutt (127). **B.** Components of infarct scar matrix are highly dynamic during the healing time-course. Curves represent the fits of reported data, averaged across a number of small animal studies after grouping into the following categories: collagen (types I, III, IV, VI) (29, 36, 39, 73, 123, 175, 182, 189, 272, 277, 292, 300), collagen cross-links (hydroxylysylpyridinium, hydroxylysylpyridinoline) (73, 175, 272, 300), provisional structure (fibrin, fibronectin, laminin) (39, 58, 139, 162, 182), matricellular proteins (tenascin-C, thrombospondin, osteopontin, periostin, SPARC) (76, 119, 144, 162, 192, 194, 237, 263), glycosaminoglycans (hyaluronan) (58), and proteoglycans (biglycan, decorin) (62, 283, 291, 300).

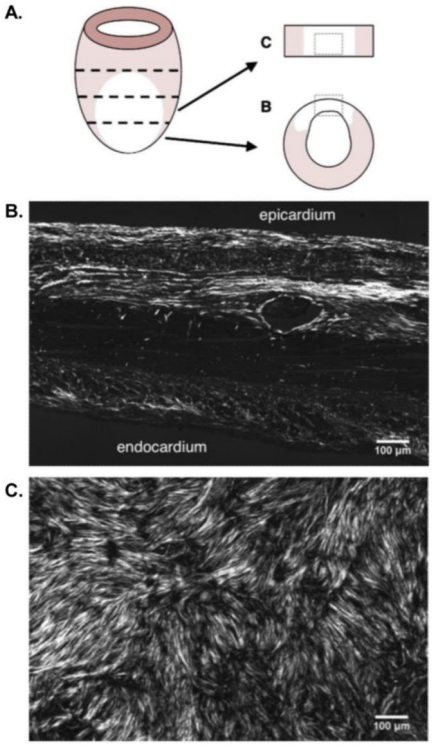

Figure 2.

Infarct collagen orientation depends on imaging plane. **A.** Infarcts are most often sectioned in the radial-circumferential (i.e., short-axis) plane, but fiber organization in the circumferential-longitudinal plane (parallel to the epicardium) is more relevant to scar mechanics. **B.** In the short-axis view, collagen fibers lie in planes parallel to the epicardium and appear to be circumferentially aligned even when the circumferential-longitudinal view (C) reveals them to be isotropic. Images are from 3-week old rat infarcts, sectioned, stained with picrosirius red, and imaged under polarized light. Reprinted with permission from Fomovsky (75).

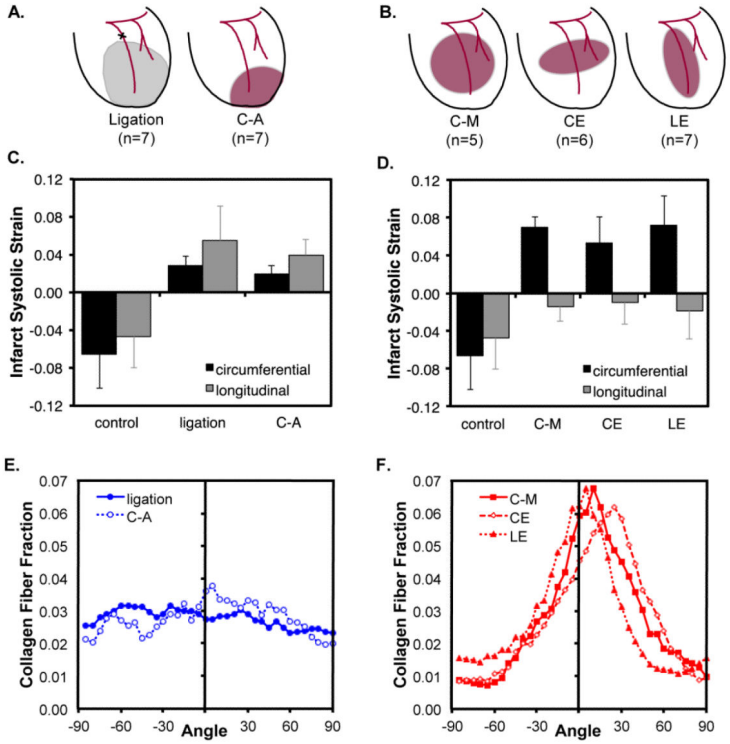

Figure 3.

Correlation between infarct mechanics and scar collagen structure in healing rat infarcts (75). **A&B.** Diagrams showing location of infarcts following permanent ligation or cryoinfarction to create infarcts with a range of shapes and locations: circular-apex (C-A), circular-midequator (C-M), circumferential ellipse (CE) at the equator, or longitudinal ellipse (LE) at the equator. **C&D.** Circumferential and longitudinal systolic strains were negative prior to infarction (control), indicating contraction. During acute ischemia, apical infarcts stretched during systole in both directions (C); by contrast, infarcts at the equator stretched only in the circumferential direction (D). **E&F.** Mean collagen orientation histograms show isotropic structure in apical infarcts (E) and circumferential alignment in equatorial infarcts (F).

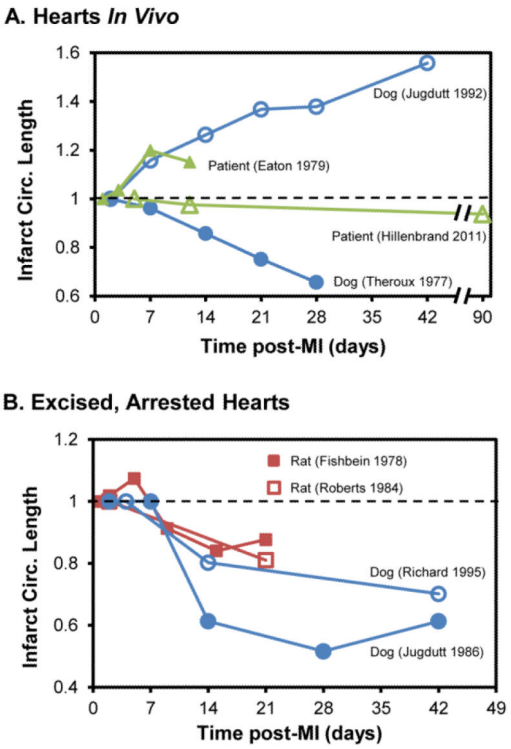

Figure 4.

Chronic infarct geometric measurements demonstrate substantial remodeling in the circumferential dimension. **A.** When assessed *in vivo*, studies sometimes report infarct expansion (increase in the scar's circumferential length) and sometimes report compaction (decrease in the scar's circumferential length). **B.** When assessed in excised, arrested hearts (i.e., no longer pressurized), studies typically report compaction. These trends are true across multiple animal models and measurement techniques.

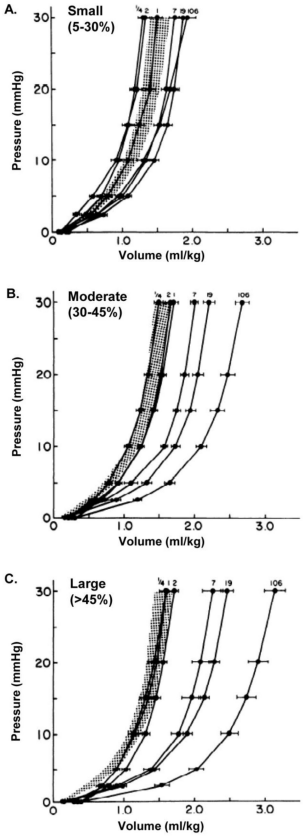

Figure 5.

Data from Pfeffer et al. on remodeling of end-diastolic pressure-volume relationship following myocardial infarction in rats (204). Following small infarcts (those affecting 5-30% of the LV circumference), effects of changes in infarct stiffness and cavity dimension offset, producing little change in the EDPVR from 6 hours (1/4 day) to 15 weeks (106 days). By contrast, substantial cavity dilation led to a progressive rightward shift of the EDPVR following larger infarcts. Small numbers at the top of each curve indicate the time post-infarction; error bars are 2*SE for group sizes of 5-10 at most time points and 12-25 at the last two time points. Figure slightly modified with permission from Pfeffer et al. (204).

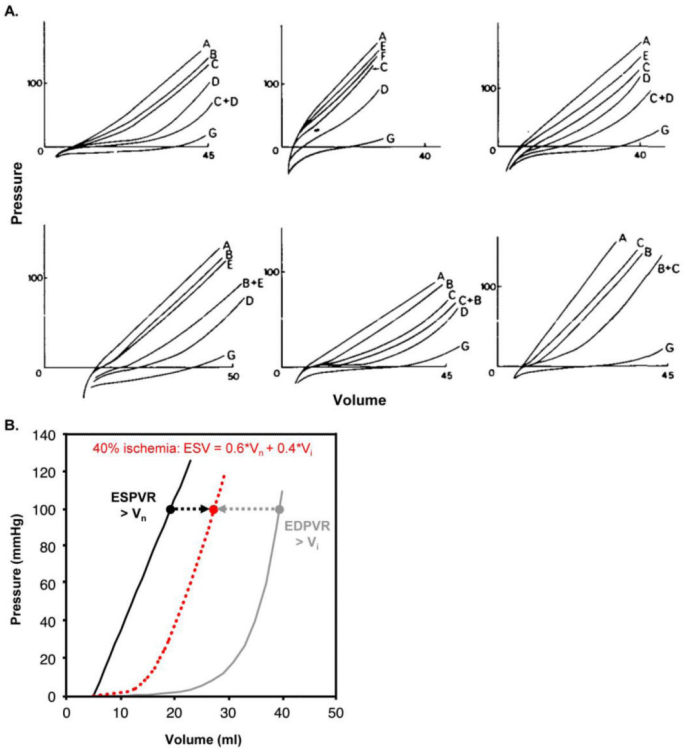

Figure 6.

Effect of acute ischemia on the end-systolic pressure-volume relationship (ESPVR). **A.** Plots from Sunagawa et al. showing a progressive rightward shift in the ESPVR as ischemic regions of increasing size were created in 6 dog hearts (reprinted with permission (251)). A – control; B – distal left circumflex (LCx) artery occlusion; C – proximal left anterior descending (LAD) artery occlusion; D – proximal LCx occlusion; E – distal LAD occlusion; F – mid-LAD occlusion; G – end-diastolic pressure volume relationship (EDPVR). **B.** Illustration of the compartmental model proposed by Sunagawa et al., for an ischemic region affecting 40% of LV mass. The model predicts the ischemic ESPVR as a weighted average of the normal ESPVR and the EDPVR, which is assumed to reflect the passive mechanical behavior of the acutely ischemic region.

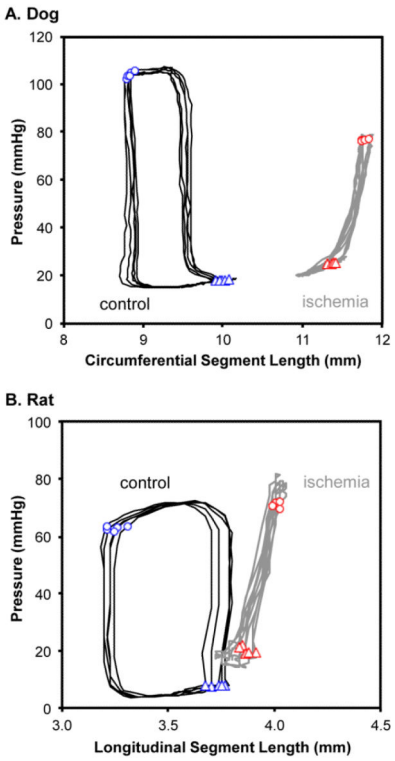

Figure 7.

Changes in pressure-segment length curves during acute ischemia. **A.** Pressure-circumferential segment length loops recorded in our laboratory from an open-chest anesthetized dog with autonomic reflexes pharmacologically blocked. Fifteen minutes of ischemia converted the active loop to an exponential, passive curve, induced a rightward shift, and increased enddiastolic pressure (EDP). **B.** Pressure-longitudinal segment length loops recorded in our laboratory from an open-chest anesthetized rat with intact autonomic reflexes. Thirty minutes of ischemia converted the active loop to a passive curve and increased EDP, shifting the segment onto a steeper region of that curve. Blue triangles – control end diastole (ED); blue circles – control end systole (ES); red triangles – ischemia ED; red circles – ischemic ES.

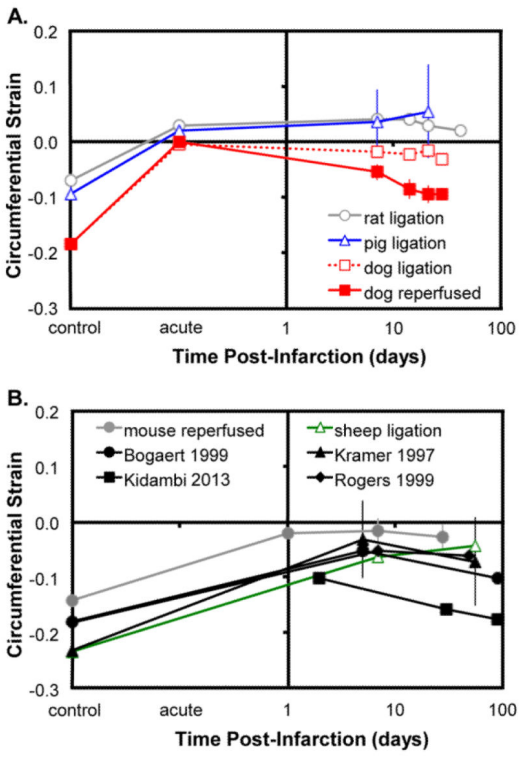

Figure 8.

Changes in regional mechanics during infarct healing. **A.** Circumferential strains reflecting deformation from end diastole to end systole measured using radiopaque markers (pig, Holmes et al. (114)) or sonomicrometers (rat, Fomovsky et al. (73); dog, Theroux et al. (258, 259)) drop to near zero acutely and remain small (usually not significantly different from zero) for several weeks after infarction in most studies. However, Theroux and coworkers found that shortening partly recovered in dogs with reperfused infarcts (closed squares), in contrast to dogs with permanent ligation studied using otherwise identical methods (open squares). **B.** Circumferential strains measured using MRI showed gradual recovery in patients with reperfused MI (black curves; (22, 136, 148, 228)) but not in mice with reperfused MI (295), or sheep with permanent ligations (147).

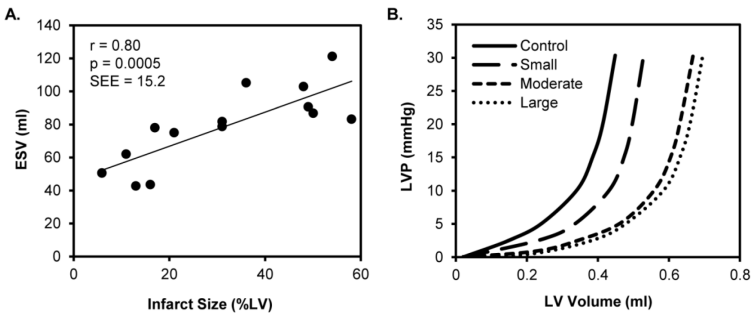

Figure 9.

Effect of infarct size on left ventricular remodeling. **A.** Measurements of LV remodeling 1 year post-MI in patients revealed that end systolic volume is linearly related to acute infarct size. Plot reprinted with permission from Chareonthaitawee et al. (41). **B.** EDPVRs of rats with a healed MI were generated by passive inflation of the arrested LV. Shifts in the average curves show that for a given LV pressure (LVP), LV cavity volume increases monotonically with infarct size. Plot reprinted with permission from Fletcher et al. (71).

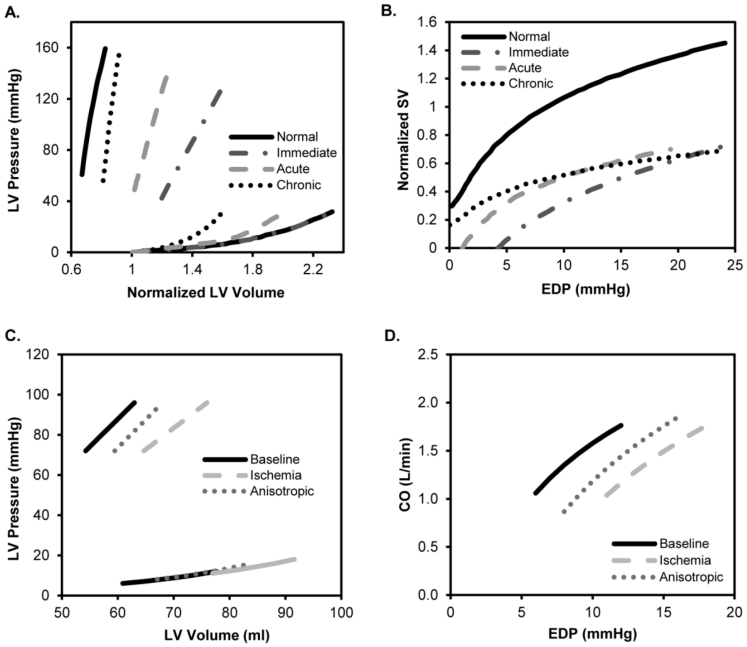

Figure 10.

Effects of infarct mechanical properties on passive and active left ventricular function. **A&B.** Original model results reprinted with permission from Bogen (23). **A.** Immediately post MI, the non-contractile ischemic area causes severe systolic dysfunction (characterized by a rightward shift in the ESPVR) with minimal effect on passive LV behavior. Systolic function improves (ESPVR shifts leftward towards baseline) as the infarct stiffens throughout healing, but the stiffer scar also impairs diastolic filling (steepening of the EDPVR). **B.** Unfortunately, similar magnitude shifts in these two curves can offset each other, leading to minimal improvement in stroke volume as the scar stiffens. **C&D.** Experimental results reprinted with permission from Fomovsky (72). **C.** Changes in passive and active LV behavior with infarction and anisotropic infarct reinforcement. Selective longitudinal reinforcement shifts the ESPVR leftward with minimal effect on the EDPVR. **D.** Anisotropic infarct reinforcement improves systolic function without impairing diastolic filling, leading to better pump function as indicated by an upward shift in the CO curve.

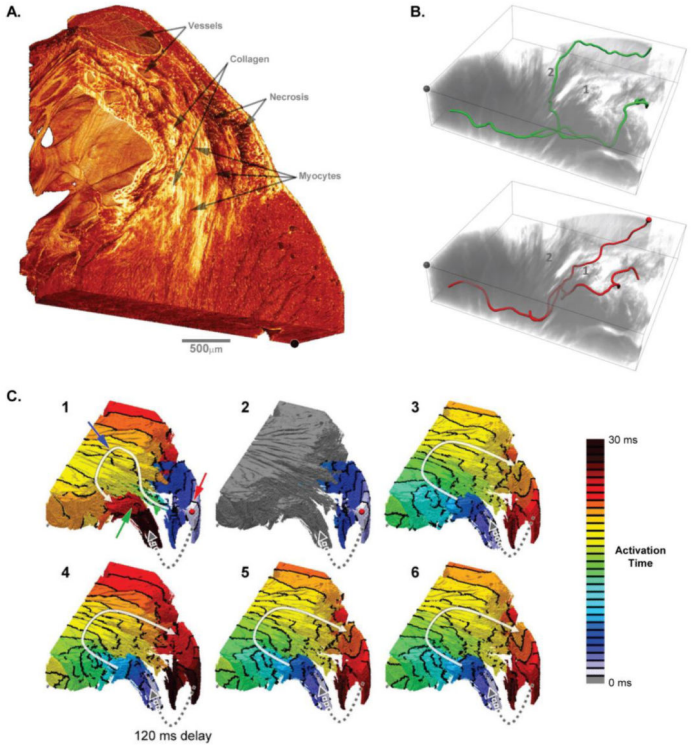

Figure 11.

A. Three-dimensional reconstruction of an infarcted region (2.99×2.68×0.70 mm^3 volume). **B.** Representative activation pathways with stimulation at the sub-endocardium (top) or sub-epicardium (bottom), demonstrating tortuous stimulus site-dependent activation pathways through the infarct. **C.** Sustained re-entry in the infarcted region induced by a stimulus train with reducing cycle length applied at the sub-epicardium (red sphere). The sub-epicardium and subendocardium were coupled at the network boundary *via* a path (dashed line) that imposed a time delay. Shown are activation maps for beats 1 to 6 (beats 1-2 were paced with a cycle length of 157 ms, then, following unidirectional block, re-entrant activation occurred in beats 3-6). The marker • indicates the basal sub-epicardium and is used as a fiducial reference. Modified with permission from Rutherford et al. (232).

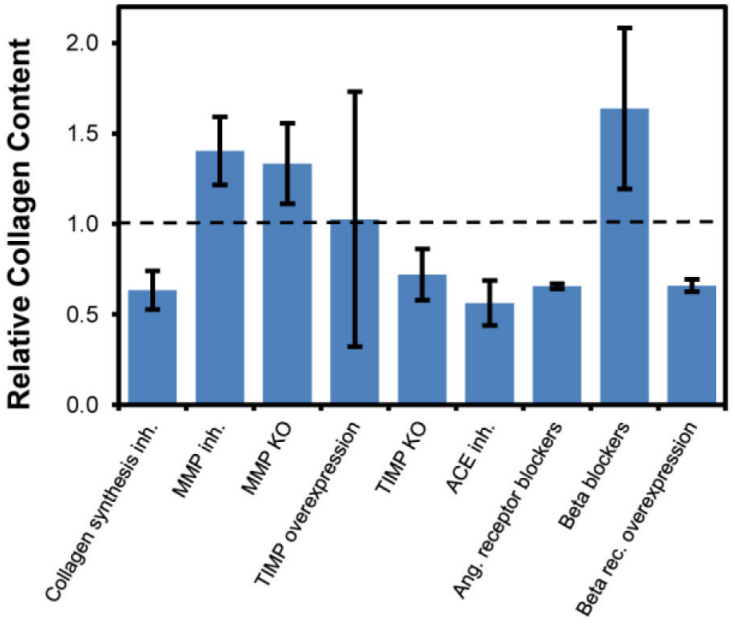

Figure 12.

Effect of various therapeutic modulations on collagen content post-myocardial infarction (post-MI). Both pharmacologic and genetic perturbations have been utilized to significantly modify the collagen content within myocardial scar. Some of these effects resulted from intentional modulation of collagen synthesis or MMP-mediated degradation within the scar (e.g., via prolyl-4-hydroxylase, MMP, or TIMP activity), while some resulted as bi-products of modulating remote cardiomyocyte signaling (e.g., via angiotensin or beta-adrenergic pathways). Bars represent means and standard deviations across available studies (see text for references).

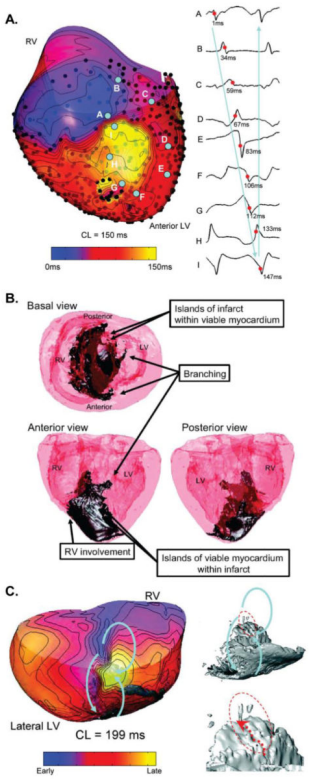

Figure 13.

A. Isochronal map generated from epicardial sock data (black dots indicate location of the electrodes) during re-entry (left) and signals from bipolar electrograms at respective locations showing progression of electrical activation traveling from point A to I (right). **B.** Three-dimensional infarct geometry reconstructed from high-resolution contrast-enhanced magnetic resonance imaging (0.39×0.39×0.39 mm spatial resolution). The infarcted region is represented by dark gray and the normal myocardium by pink. Islands of viable myocardium within the scar, as well as islands of scar within the viable myocardium, are present. **C.** Combined electrical and structural data showing the re-entrant isthmus located at the postero-apical segment of the infarcted region (circumscribed by a broken red line). The scar geometry at the isthmus was characterized by scar tissue interspersed with multiple tracts of viable myocardium. Possible electrical propagation at the infarct border-zone is indicated by the dashed red arrow. Modified with permission from Ashikaga et al. (6).

Table 1

Potential confounders of functional measures following myocardial infarction; each row indicates a functional measure, with an 'x' in the columns showing factors that directly affect it. Most available indices of diastolic, systolic, and overall pump function are also affected by LV dilation, infarct size and material properties, making evaluation of intrinsic LV function quite challenging. The least confounded measures of diastolic (EDPVR), systolic (ESPVR), and global (CO curve) function are curves constructed from data at multiple levels of preload/afterload; given these curves, appropriate models can help account for effects of variations in LV geometry and infarct size/stiffness. The two most widely used indices – stroke volume (SV) and ejection fraction (EF) – are also the most difficult to interpret. Contractility refers to contractility of surviving viable myocardium, EDV = end-diastolic volume, EDPVR = end-diastolic pressure-volume relationship, ESV = end-systolic volume, dP/dtmax = maximum rate of pressure generation, ESPVR Emax = slope of end-systolic pressure-volume relationship, ESPVR V0 = intercept of end-systolic pressure-volume relationship, CO = cardiac output.

Measure	Infarct Size	Infarct Stiffness	Contractility	Preload	Afterload	LV Dilation
EDV	x	x		x		x
EDPVR	x	x				x
ESV	x	x	x	x	x	x
dP/dt_{max}	x	x	x	x		x
ESPVR E_{max}		x	x			x
ESPVR V_0	x	x				x
SV	x	x	x	x	x	x
CO	x	x	x	x	x	x
CO curve	x		x		x	x
EF	x	x	x	x	x	x

Table 2

Effects of mechanical interventions on cardiac remodeling and function post-MI. A variety of global restraint, local restraint, and intramural material injection approaches have been used in attempts to limit infarct and LV remodeling, improve LV function, or both. In general, global restraint has been most effective in limiting LV remodeling, followed by local restraint, then intramural injection. Few of these therapies have convincingly improved LV function acutely, but those that reduce remodeling can also limit functional decline associated with that remodeling. Despite the fact that injectable therapies have provided less benefit, their clinical delivery is potentially much less invasive. Reported increases or decreases signify a statistically significant change from the MI sham-therapy group. OQVR = Optimized Quantitative Ventricular Restraint, AMVR = Adjustable and Measureable Ventricular Restraint, PP = polypropylene, MSCs = mesenchymal stem cells, PLGA = poly(lactic-co-glycolic) acid, EHT = Engineered Heart Tissue, PEUU = polyester urethane urea, PGCL = poly(glycolide-co-caprolactone), BMCs = bone marrow cells, PTFE = polytetrafluoroethylene, PU = polyurethane, myo = decellularized myocardium, PEG = poly(ethylene glycol), MeHA = methacrylated hyluronic acid. (20, 21, 40, 42, 54, 60, 72, 78, 85, 87, 90, 91, 98, 118, 129–131, 133, 134, 152, 153, 155, 158, 166, 174, 180, 186, 208, 209, 212, 218, 233, 242, 301)

Reference	Species	Disease Model	Therapy	Timing	EDV	ESV	EF	SV	CO	FS/FAS/WT	dP/dt	ESPVR
Global Restraints												
Power 1999	sheep	rapid pacing HF	CorCap	after 3wks of pacing				↔	↔	↑FS	↔	
Chaudry 2000	dog	microembolization HF	CorCap	2wks	↓					↑FAS		
Pilla 2005	sheep	LAD ligation	CorCap	1wk	↓	↓				↑WT in BZ		
Blom 2005	sheep	LAD ligation	CorCap	1wk	↓	↓	↑	↔				
Blom 2007	sheep	LAD ligation	CorCap	1wk	↓	↓	↑			↑radial strain in BZ		
George 2007	dog	microembolization HF	HeartNet	after developing HF	↓	↓						
Magovern 2006	sheep	LAD ligation	HeartNet	immediate	↓	↓	↔	↔	↔			
McCarthy 2001	dog	rapid pacing HF	Myosplint	after developing HF	↓	↓	↑	↔	↔			
Guccione 2003	human	FEM of global dilation	Myosplint	after developing HF	↓	↓			↔			↑
Kashem 2002	dog	rapid pacing HF	CardioClasp	after developing HF						↑FAC		↑PSLR
Kashem 2003a	dog	rapid pacing HF	CardioClasp	after developing HF					↔		↔	↑PAR
Kashem 2003b	dog	rapid pacing HF	CardioClasp	after developing HF	↓CSA	↓CSA						↑
Ghanta 2007	sheep	LAD diagonal ligation	OQVR	immediate	↓		↑					
Lee 2012	sheep	LAD diagonal ligation	AMVR	immediate	↓	↓	↑					
Local Restraints												
Kelley 1999	sheep	LAD ligation	PP	pre-MI	↓	↓	↑	↑	↑			↑
Moainie 2002	sheep	LCx ligation	PP	pre-MI	↔	↔	↔	↔	↔			

Reference	Species	Disease Model	Therapy	Timing	EDV	ESV	EF	SV	CO	FS/FAS/WT	dP/dt	ESPVR
Liu 2004	pig	60min LAD occlusion	fibrin + MSCs	immediate						↑WT in infarct		
Kellar 2006	mouse	LAD ligation	PLGA + fibroblasts	immediate		↓	↑	↔	↔			↔
Zimmermann 2006	rat	LAD ligation	EHT	2wks	↔	↔	↔	↔	↔	↔FAS	↔	
Fujimoto 2007	rat	LAD ligation	PEUU	2wks	↓					↑FAC		
Simpson 2007	rat	LAD ligation	collagen + MSCs	immediate	↓	↓				↑FS	↔	
Piao 2007	rat	5hrs LAD occlusion	PGCL + BMCs	1wk	↓EDD	↓ESD				↑FS		
Chachques 2008	human	post-ischemic scars	collagen + BMCs	N/A	↓	↓	↔					
Liao 2010	pig	LCx embolization	PP + PTFE	8wks	↓	↓	↑				↑	
Giraud 2010	rat	LAD ligation	PU + myoblasts	2wks	↑EDD					↓FS	↔	
Godier-fumemont 2011	rat	LAD ligation	myo + fibrin + MSCs	immediate	↓EDD	↓ESD				↑FS		
Fomovsky 2012	dog	LAD ligation	anisotropic dacron	immediate		↓			↑			
Intramural Injections												
Dai 2005	rat	LAD ligation	collagen	1wk	↔	↔	↑	↑				
Landa 2008	ra	LAD ligation	alginate	1wk	↓	↓				↔FS, FAC		
				6wks	↔	↔				↔FS, FAC		
Mukherjee 2008	pig	OM ligation	fibrin-alginate	1wk	↔		↔				↔	
Ryan 2009	sheep	LAD ligation	Radiesse®	immediate	↓	↓	↑		↑			
Dobner 2009	rat	LAD ligation	PEG	immediate	↔	↔				↔FS		
Leor 2009	pig	90 min LAD occlusion	alginate	3d	↓	↓				↔FS		
Ifkovits 2010	sheep	LAD ligation	MeHA (l)	immediate	↔	↔	↔		↔			
			MeHA (h)		↔	↔	↔		↔			
Rane 2011	rat	LAD ligation	PEG	9d	↔	↔	↔					

Compr Physiol. Author manuscript; available in PMC 2016 October 01.